

See discussions, stats, and author profiles for this publication at: <https://www.researchgate.net/publication/6951218>

# First Principle Computational Study on the Full Conformational Space of l-Proline Diamides

ARTICLE in THE JOURNAL OF PHYSICAL CHEMISTRY A · APRIL 2005

Impact Factor: 2.69 · DOI: 10.1021/jp040594i · Source: PubMed

CITATIONS

27

READS

28

9 AUTHORS, INCLUDING:



**Tara Kehoe**

University of Toronto

21 PUBLICATIONS 804 CITATIONS

SEE PROFILE



**Gregory Chass**

Queen Mary, University of London

105 PUBLICATIONS 1,325 CITATIONS

SEE PROFILE



**Botond Penke**

University of Szeged

379 PUBLICATIONS 7,906 CITATIONS

SEE PROFILE



**Emil F Pai**

University of Toronto

201 PUBLICATIONS 10,648 CITATIONS

SEE PROFILE

# First Principle Computational Study on the Full Conformational Space of L-Proline Diamides

Michelle A. Sahai,<sup>\*,†,‡,§,||</sup> Tara A. K. Kehoe,<sup>‡,§,⊥</sup> Joseph C. P. Koo,<sup>‡,§,#</sup> David H. Setiadi,<sup>‡,§,||</sup> Gregory A. Chass,<sup>‡,§,⊗,♦</sup> Bela Viskolcz,<sup>||</sup> Botond Penke,<sup>||,‡</sup> Emil F. Pai,<sup>†</sup> and Imre G. Csizmadia<sup>\*,‡,§,||,⊗</sup>

Department of Medical Biophysics, University of Toronto, Ontario Cancer Institute, Princess Margaret Hospital, 610 University Avenue, Toronto, Ontario, Canada M5G 2M9, Department of Chemistry, University of Toronto, 80 St. George Street, Toronto, Ontario, Canada M5S 3H6, Global Institute of Computational Molecular and Materials Science (GIOCOMMS), 1422 Edenrose St., Mississauga, Ontario, Canada L5V 1H3, Department of Medical Chemistry, University of Szeged, Dóm tér 8, Szeged, Hungary 6720, Bolyai Institute, University of Szeged, Aradi Vértanúk Tere 1, Szeged, Hungary 6720, Department of Pharmaceutical Sciences and Institutes of Drug Research, University of Toronto, 19 Russell Street, Toronto, Ontario, Canada M5S 2S2, Instituto de Biocomputación y Física de los Sistemas Complejos (BIFI), Edificio Cervantes, Corona de Aragón 42, Zaragoza, Spain 50009, Departamento de Física Teórica, Facultad de Ciencias, Universidad de Zaragoza, Pedro Cerbuna 12, Zaragoza, Spain 50009, Department of Chemistry and Chemical Informatics, University of Szeged, Boldogasszony sgt. 6, Szeged, Hungary 6725, Protein Chemistry Research Group, Hungarian Academy of Sciences, University of Szeged, Dóm tér 8, Szeged, Hungary 6720, Department of Organic Chemistry, University of Szeged, Dóm tér 8, Szeged, Hungary 6720

Received: September 1, 2004; In Final Form: December 27, 2004

Ab initio molecular orbital computations were carried out at three levels of theory: RHF/3-21G, RHF/6-31G(d), and B3LYP/6-31G(d), on four model systems of the amino acid proline, HCO–Pro–NH<sub>2</sub> [I], HCO–Pro–NH–Me [II], MeCO–Pro–NH<sub>2</sub> [III], and MeCO–Pro–NH–Me [IV], representing a systematic variation in the protecting N- and C-terminal groups. Three previously located backbone conformations,  $\gamma_L$ ,  $\epsilon_L$ , and  $\alpha_L$ , were characterized together with two ring-puckered forms syn (gauche<sup>+</sup> = g<sup>+</sup>) or “DOWN” and anti (gauche<sup>–</sup> = g<sup>–</sup>) or “UP”, as well as trans–trans, trans–cis, cis–trans, and cis–cis peptide bond isomers. The topologies of the conformational potential energy cross-sections (PECS) of the potential energy hypersurfaces (PEHS) for compounds [I]–[IV] were explored and analyzed in terms of potential energy curves (PEC), and HCO–Pro–NH<sub>2</sub> [I] was also analyzed in terms of potential energy surfaces (PESs). Thermodynamic functions were also calculated for HCO–Pro–NH<sub>2</sub> [I] at the CBS-4M and G3MP2 levels of theory. The study confirms that the use of the simplest model, compound [I] with P<sub>N</sub> = P<sub>C</sub> = H, along with the RHF/3-21G level of theory, is an acceptable practice for the analysis of peptide models because only minor differences in geometry and stability are observed.

## 1. Introduction

### 1.1. Rationale for the First Principle Computational Study.

Proline (Pro), a cyclic aliphatic amino acid, is a major component of the protein collagen<sup>1</sup> found in connective tissues and is incorporated into other proteins at a rate of approximately 4% with respect to all other amino acids.<sup>2–4</sup> Due to the rigid nature of its five-membered pyrrolidine side chain (SC) ring,

the presence of proline residues in biomolecules limits the flexibility of chain formation.<sup>5</sup> This may also account for proline's positional preference at the beginning of  $\alpha$ -helices,<sup>6,7</sup> forming kinked  $\alpha$ -helical structures.<sup>8</sup> Structural studies show proline frequently stabilizes  $\beta$ -turns<sup>9,10</sup> and  $\gamma$ -turns.<sup>11,12</sup> In the cell, proline residues are important not only in the formation of helices but also in receptor oligomerization,<sup>13</sup> receptor activation, and ligand binding.<sup>14</sup> Proline also reduces nonspecific proteolytic degradation in a peptide chain.<sup>15</sup>

All amino acid residues, including proline, are important in determining secondary structure and tertiary structure. Numerous studies have already been conducted on the geometry of proline, with emphasis not only on its limited backbone (BB) conformers but also on the rigid nature of its five-membered pyrrolidine SC ring, which significantly determines its role in protein structure and function. The structural features relating to the conformational behavior of proline originated from both experimental techniques such as X-ray crystallography,<sup>16–21</sup> NMR,<sup>22–25</sup> IR spectroscopy,<sup>26,27</sup> and theoretical calculations including semiempirical force-field studies<sup>28–32</sup> and electronic structure methods employing ab initio and density functional theory (DFT).<sup>33–49</sup>

\* Corresponding authors. E-mail: M.A.S., michelle.sahai@utoronto.ca; I.G.C., icsizmad@jgytf.u-szeged.hu.

<sup>†</sup> Department of Medical Biophysics, University of Toronto.

<sup>‡</sup> Department of Chemistry, University of Toronto.

<sup>§</sup> Global Institute of Computational Molecular and Materials Science.

<sup>||</sup> Department of Medical Chemistry, University of Szeged.

<sup>⊥</sup> Bolyai Institute, University of Szeged.

<sup>#</sup> Department of Pharmaceutical Sciences and Institutes of Drug Research, University of Toronto.

<sup>⊗</sup> Instituto de Biocomputación y Física de los Sistemas Complejos (BIFI).

<sup>♦</sup> Departamento de Física Teórica, Facultad de Ciencias, Universidad de Zaragoza.

<sup>†</sup> Department of Chemistry and Chemical Informatics, University of Szeged.

<sup>‡</sup> Protein Chemistry Research Group, Hungarian Academy of Sciences, University of Szeged.

<sup>⊗</sup> Department of Organic Chemistry, University of Szeged.

The majority of these theoretical studies included structural investigations of the free parent amino acid proline and its side chain pyrrolidine ring, but no study to date has allowed for variation in the N- and C-terminally protected proline diamide ( $\text{HCO-Pro-NH}_2$  [I],  $\text{MeCO-Pro-NH}_2$  [II],  $\text{HCO-Pro-NH-Me}$  [III], and  $\text{MeCO-Pro-NH-Me}$  [IV]) to investigate the subsequent effects on the geometry of the parent amino acid proline. The implications of such a study are valuable, considering that proline does not exist by itself in proteins but is flanked both on the N- and C-terminal sides by other amino acid residues, including selenocysteine (Sec). Such a study would seek to explicitly mimic the nearest-neighboring residues of the polypeptide chain and any steric and electronic effects they may impose upon the proline residue.

It has been established that a database consisting of all theoretically possible conformations of N- and C-terminally protected amino acid diamides, previously optimized using ab initio QM methods, may facilitate the application of multidimensional conformational analysis (MDCA).<sup>50–55</sup> By applying established methods,<sup>53–54</sup> nonexistent conformations could be eliminated and established structures could be used as inputs for the optimization of larger systems. Inputs can then be built up by extracting the internal coordinates of re-optimized amino acid residues. This can be readily done using a recently introduced modular numbering of the atomic nuclei.<sup>53,54</sup> Even though this method does not take into account the structure-stabilizing role of long-range interactions and the effect of solvation, it is still possible to obtain a wealth of structural and electronic information of the conformers populated, based only on the conformational preference<sup>56–59</sup> of single amino acid residues.

Therefore, the precomputed amino acid structure of proline would be important for future investigations of larger oligopeptides, such as  $\text{Pro-Pro-Thr-Pro}$  and  $\text{Pro-Pro-Gly-Phe}$  occurring as significant tetrapeptide segments in the antibody Immunoglobulin A1 (IgA1)<sup>60,61</sup> and Bradykinin,<sup>62,63</sup> respectively. The authors do recognize that any larger structure making use of precomputed data would have to undergo a geometry optimization once again; however, it has been shown that use of precomputed data affords a more optimal input structure, increasing computational and methodological efficiency.<sup>54</sup>

**1.2. Structural Considerations for First Principle Computational Study.** Given that the backbone of any amino acid residue in a peptide or a protein may be considered as a triple rotor (Figure 1a), the torsional angles,  $\phi_i$ ,  $\psi_i$ , and  $\omega_i$ , allow for characterization of the rotation about the N–C, the C–CO, and the OC–NH (i.e., the peptide) bonds, respectively. Consequently, the energy associated solely with BB conformational change would lead to a potential energy hypersurface (PEHS) of the following form:

$$E = f(\phi_i, \psi_i, \omega_i) \quad (1)$$

The general orientation of a peptide side chain is predetermined by the rotation about the  $\text{C}^\alpha\text{--C}^\beta$  single bond denoted as  $\chi_i^1$ . Further side chain torsions ( $\chi_i^j$ ) may be defined depending on the length of the side chain. As Figure 1a (side view) suggests,  $\phi_i$ ,  $\psi_i$ , and  $\chi_i^1$  may be coupled substantially,<sup>64</sup> as they describe the internal rotation of functional groups located on the geminally substituted  $\alpha$ -carbon atom. Thus, considering only trans peptide bonds ( $\omega_{i-1} = 180^\circ$  and  $\omega_i = 180^\circ$ ) a single amino acid residue is governed by a PEHS as shown in (2), rather than the more commonly studied potential energy surface (PES).

$$E = f(\phi_i, \psi_i, \chi_i^1) \quad (2)$$

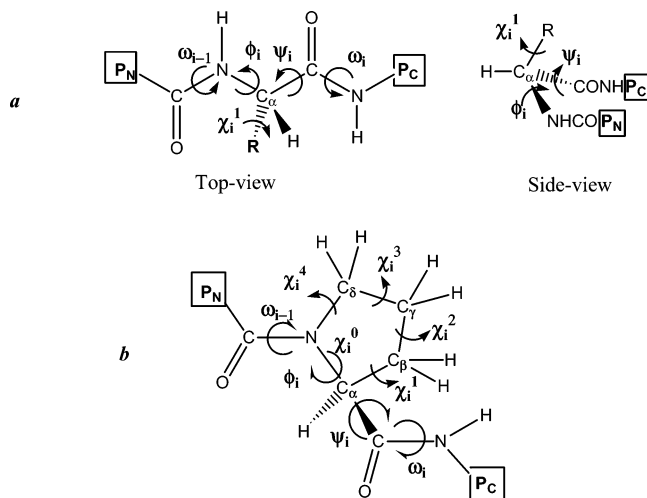


**Figure 1.** Schematic illustration of (a) a general amino acid with side chain R and (b) the amino acid residue proline, showing the characteristic torsional angles  $\omega_{i-1}$ ,  $\omega_i$ ,  $\phi_i$ ,  $\psi_i$ , and  $\chi_i^1$ . The protecting end groups used in this study,  $P_C$  and  $P_N$  are also illustrated; where  $P_N$  and  $P_C$  denote H and  $\text{CH}_3$ .

The only exception to this rule is glycine, in which  $R = \text{H}$  has the following energetic description:

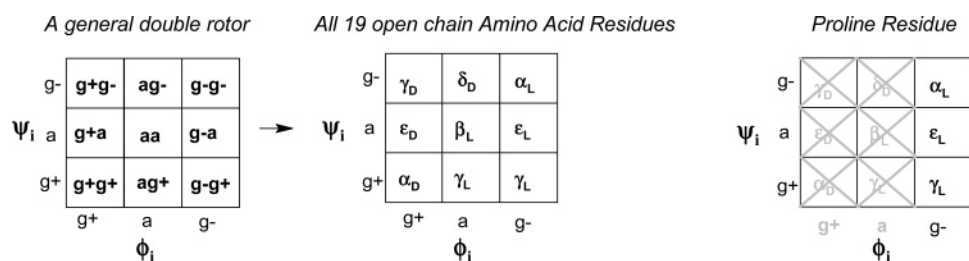
$$E = f(\phi_i, \psi_i) \quad (3)$$

The situation is further complicated if the amino acid residue is proline. As illustrated in Figure 1b, the side chain R group of a proline residue forms a five-membered ring with the backbone. One may consider that proline is essentially an amino acid with its nitrogen situated in a pyrrolidine ring. Because the already defined  $\phi_i$  backbone torsion is contained within the five-membered ring, it has been shown that possible stable structures of the proline residue may only exist, almost exclusively, in the  $\gamma_L$ ,  $\epsilon_L$ , and  $\alpha_L$  backbone conformations as only  $\psi_i$  is an unrestrained, and therefore continuous, variable.<sup>35</sup> Consequently, it is not trivial to obtain conformational information about the proline residue either theoretically or experimentally.

Proline side chains can adopt two different conformational states denoted by either syn ( $\text{gauche}^+ = g^+$ ) or anti ( $\text{gauche}^- = g^-$ ), which correspond to “DOWN” or “UP” ring puckerings, respectively.<sup>21,31</sup> Regardless of the terminology used to identify the ring pucker, the differences can be identified by considering the distribution of proline side chain dihedral angles. In particular, syn ( $\text{gauche}^+ = g^+$ ) or “DOWN” ring pucker is characterized by positive values of  $\chi_i^1$  and  $\chi_i^3$  and negative values of  $\chi_i^2$  and  $\chi_i^4$ . Accordingly, anti ( $\text{gauche}^- = g^-$ ) or “UP” ring pucker is characterized by negative values of  $\chi_i^1$  and  $\chi_i^3$  and positive values of  $\chi_i^2$  and  $\chi_i^4$ . This paper makes use of the simplified notation for representing ring pucker whereby syn ( $\chi_i^1 = g^+$ ) represents “DOWN” ring pucker, and anti ( $\chi_i^1 = g^-$ ) represents “UP” ring pucker.

In its neutral form, the proline residue has no peptidic N–H group that may act as an H-bond donor.<sup>35</sup> It has been shown that when proline is N-protonated, the global minimum of the proline residue assumes the syn ( $\chi_i^1 = g^+$ ) or “DOWN” conformation as a cis isomer whereas the structure is stabilized by an intramolecular hydrogen bond.<sup>37</sup> As there are two carbon atoms connected to the pyrrolidine nitrogen, the stability of the proline residue may be highly dependent on cis/trans isomerization of the peptide bond, in conjunction with the existence of syn ( $\chi_i^1 = g^+$ ) or “DOWN” and anti ( $\chi_i^1 = g^-$ ) or “UP” pucker in the ring.

## SCHEME 1



Although the pyrrolidine ring is considered to permit only one  $\phi_i$  value in the vicinity of the gauche<sup>-</sup> ( $g^-$ ) (i.e.,  $\phi_i = -60^\circ$ ),  $\psi_i$  may assume three different “poses” in the vicinity of gauche<sup>+</sup> ( $g^+$ ); (i.e.,  $\psi_i = 60^\circ$ ), anti ( $a$ ); (i.e.,  $\psi_i = 180^\circ$ ) and gauche<sup>-</sup> ( $g^-$ ); (i.e.,  $\psi_i = -60^\circ$ ), corresponding to  $\gamma_L$ ,  $\epsilon_L$ , and  $\alpha_L$  conformers, respectively. Therefore, rather than the nine MDCA-predicted conformers,<sup>52</sup> as indicated in Scheme 1, only three discrete conformers corresponding to  $\gamma_L$ ,  $\epsilon_L$ , and  $\alpha_L$  may be expected for the proline residue.<sup>35</sup>

Thus,  $\phi_i$  may be regarded as a static parameter, whereby the typical Ramachandran PES of type (3) becomes a Ramachandran potential energy curve (PEC) of type (4) for the proline residue.

$$E = f(\psi_i) \quad (4)$$

Only the traditional PEC (4), a cross-section of the full Ramachandran type PES (3), was previously calculated<sup>35</sup> for HCO-Pro-NH<sub>2</sub> for the trans peptide bond with  $\omega_{i-1}$  optimized at about  $180^\circ$ . In addition, the puckering patterns of proline were also previously reported.<sup>33-49,65,66</sup>

The peptide bond can theoretically assume a cis or a trans configuration, with  $\omega$  values in the vicinity of  $0^\circ$  or  $180^\circ$ , respectively. A cis  $\omega$  peptide bond following a proline residue is only biochemically significant for oligoproline and polypeptides,<sup>65,66</sup> thus justifying the scope of the present study whereby a proline database consisting of all theoretically possible conformations may be instrumental in efficient investigation of larger oligopeptides containing proline. Therefore, as a single amino acid diamide residue, the  $\omega_{i-1}$  and  $\omega_i$  torsions for proline could lead, in principle, to trans-trans, trans-cis, cis-trans, or cis-cis configurations (Figure 2).

Consequently, in this study, we wish to explore, characterize, and present the geometric preferences of HCO-Pro-NH<sub>2</sub> [I], MeCO-Pro-NH<sub>2</sub> [II], HCO-Pro-NH-Me [III], and MeCO-Pro-NH-Me [IV] (hereinafter referred to as the P<sub>N</sub>-CO-Pro-NH-P<sub>C</sub> family) developed for both cis and trans isomers (Figure 2).

## 2. Method

**2.1. Standardized Input Files.** Numeric definitions of the relative spatial orientation of all constituent atoms of the P<sub>N</sub>-CO-Pro-NH-P<sub>C</sub> systems follows an established standard,<sup>53,54</sup> shown explicitly in Figure 3. The proline residue as well as the protecting end groups is therefore exclusively defined. The *Gaussian 03* program package,<sup>67</sup> was used in all computations of this work.

**2.2. Calculating Pseudorotational Parameters for the P<sub>N</sub>-CO-Pro-NH-P<sub>C</sub> Family.** The concept of pseudorotation first introduced by Kilpatrick et al.<sup>68</sup> has been examined extensively by many previous experimental and theoretical methods.<sup>19,33,38,39,69-79</sup> The concept of pseudorotation describes a method of representing the conformations of five-membered saturated rings, which are likely to be puckered (e.g., the cyclopentane ring and the pyrrolidine ring of proline) in contrast to aromatic rings (i.e., pyrrole), which are planar.<sup>43</sup> According to this concept, because the ring is flexible, the maximum puckering rotates around the ring adopting the “envelope”, “twist”, and “half-twist” forms, with minor interference to energy barriers.<sup>42,73</sup> For the pyrrolidine ring, these barriers were

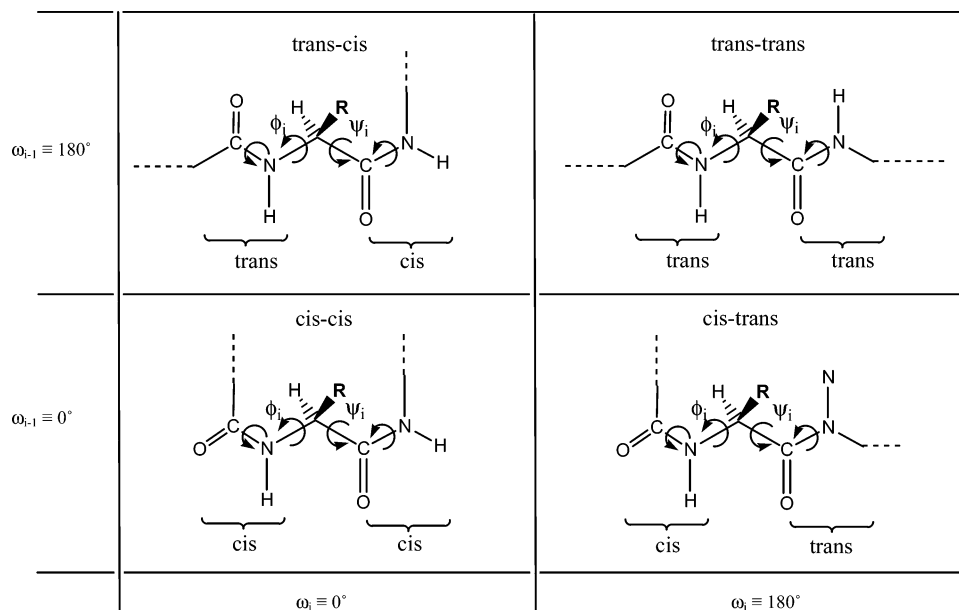


**Figure 2.** Schematic illustration of the characteristic  $\omega_{i-1}$  and  $\omega_i$  torsions for proline leading to trans-trans, trans-cis, cis-trans, or cis-cis configurations.

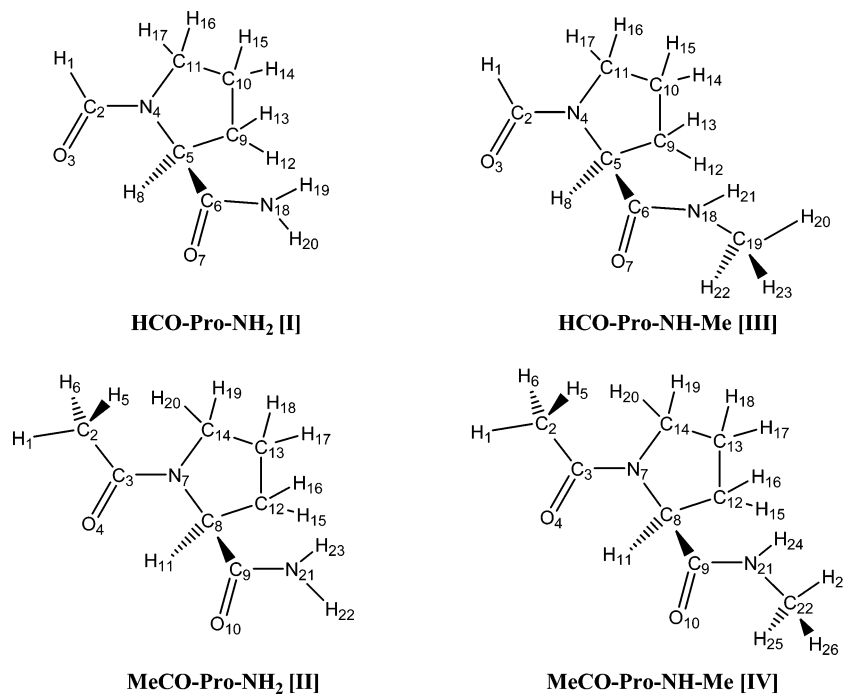


**Figure 3.** Schematic illustration of the numbering system applied to the amino acid diamides HCO-Pro-NH<sub>2</sub> [I], MeCO-Pro-NH<sub>2</sub> [II], HCO-Pro-NH-Me [III], and MeCO-Pro-NH-Me [IV].

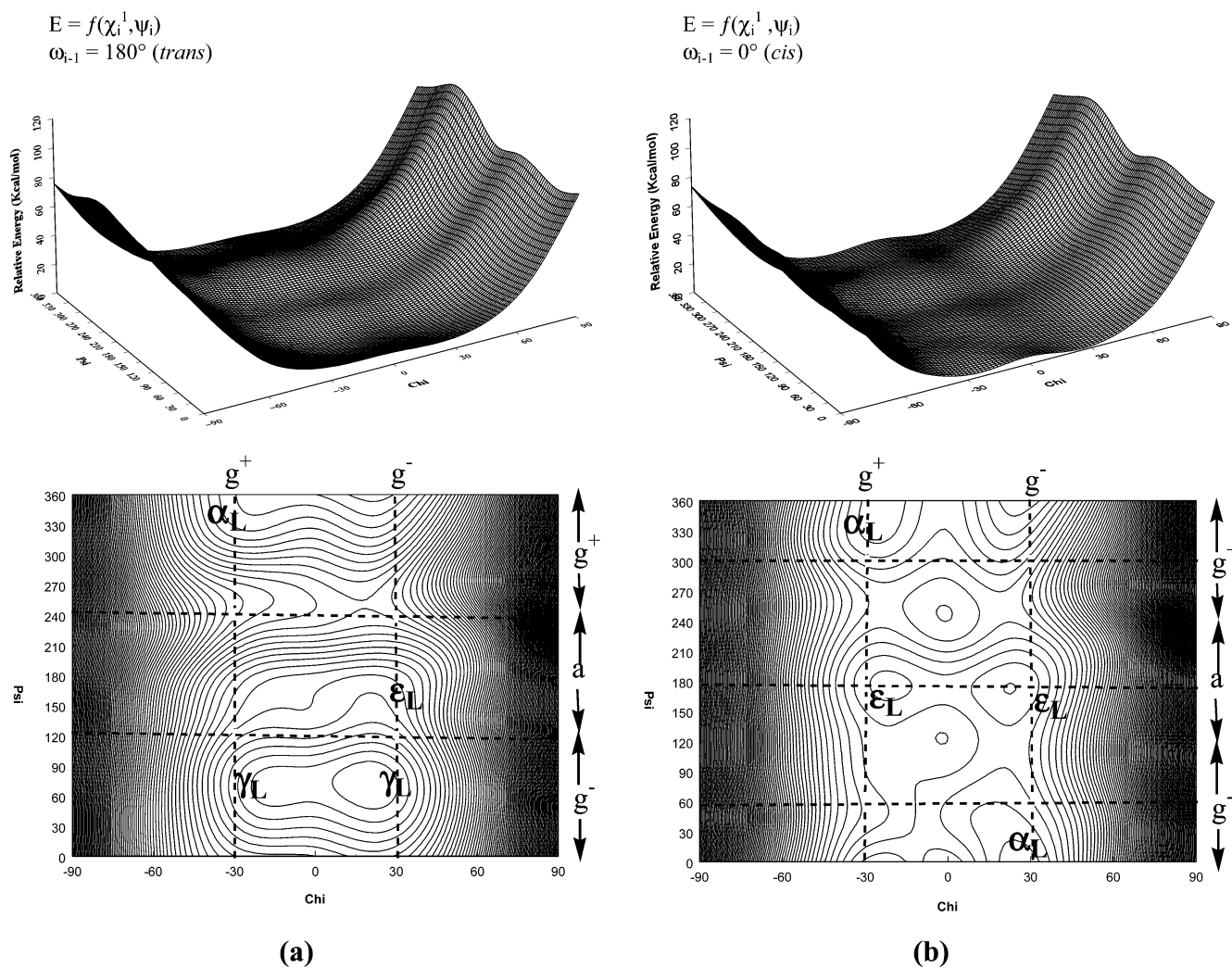
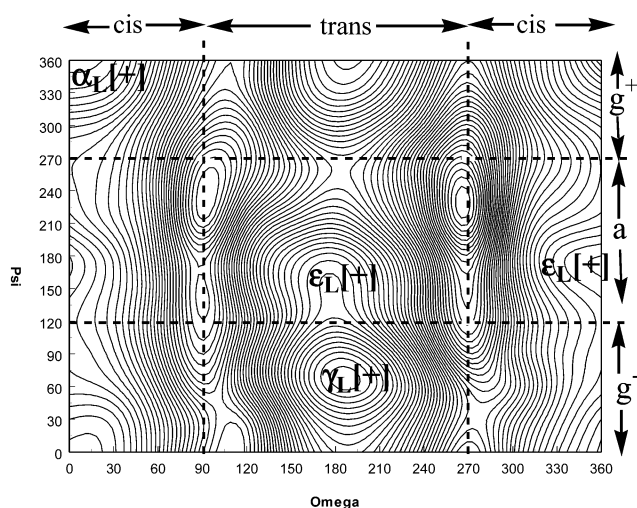
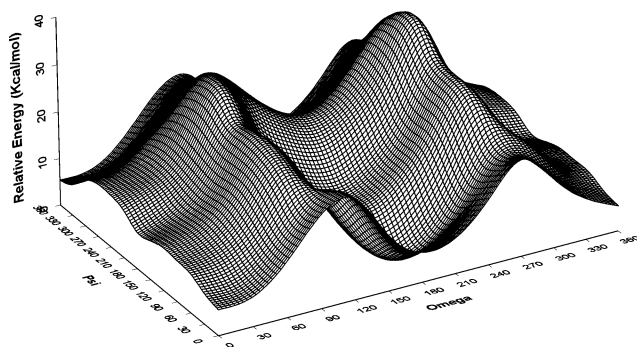


**Figure 4.** Potential energy hypersurface landscape (top) and contour map (bottom) of (a) HCO-Pro-NH<sub>2</sub> for  $E = f(\chi_i^1, \psi_i)$  at  $\omega_{i-1} = 180^\circ$  (*trans*) and (b) HCO-Pro-NH<sub>2</sub> for  $E = f(\chi_i^1, \psi_i)$  at  $\omega_{i-1} = 0^\circ$  (*cis*).



$$E = f(\omega_i, \psi_i)$$

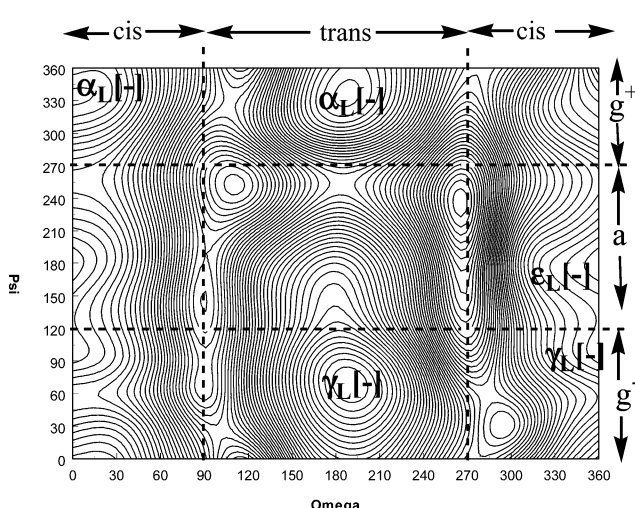
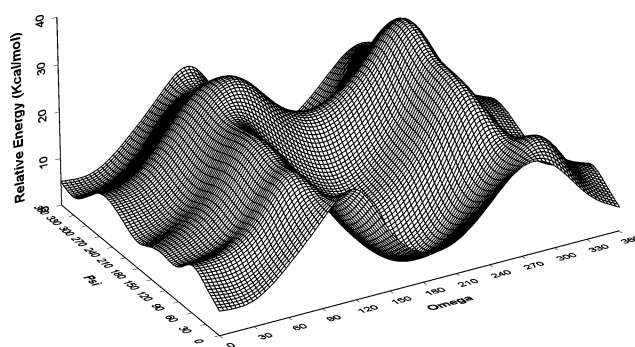
$$\chi_i^1 = g^+$$



(a)

$$E = f(\omega_i, \psi_i)$$

$$\chi_i^1 = g^-$$



(b)

**Figure 5.** Potential energy surface landscape (top) and contour map (bottom) of (a) HCO-Pro-NH<sub>2</sub> for  $E = f(\omega_i, \psi_i)$  at  $\chi_i^1 = g^+$  and (b) HCO-Pro-NH<sub>2</sub> for  $E = f(\omega_i, \psi_i)$  at  $\chi_i^1 = g^-$ .

**TABLE 1: Schematic Topological Pattern of Occurrence of Minimum Energy Conformers of Compounds [I] and [II] at the RHF/3-21G Level of Theory**

SC	BB	trans		cis	
		I	II	I	II
$g^+$	$\alpha_L$				
	$\epsilon_L$	✓	✓	✓	✓
	$\gamma_L$	✓	✓		
$g^-$	$\alpha_L$	✓	✓	✓	✓
	$\epsilon_L$			✓	✓
	$\gamma_L$	✓	✓		

estimated to be on the order of 2–4 kJ·mol<sup>-1</sup> on the basis of electronic structure methods.<sup>74,77,78</sup>

Many parameters of pseudorotation have been defined. Kilpatrick et al.<sup>68</sup> and the improvements proposed by Cremer and Pople<sup>72</sup> describe the puckering of cyclopentane by pseudorotation on the basis of the displacements of each atom perpendicular to the mean plane of the ring. Following the use of endocyclic torsion angles,<sup>69</sup> which precluded the need to define the mean plane, it was shown that in the case of infinitesimal displacements of a pentagon from planarity, there is a direct linear relationship between the torsion angles and displacements.<sup>71</sup> These parameters were found to be related to those in the original definitions;<sup>68</sup> however, finite displacements deviate from these linear relationships.<sup>71</sup> The concept of pseudorotation has been further modified by introducing correction terms for describing nonequilateral rings.<sup>76</sup>

In this work, the concept of pseudorotation is used to describe the puckering of the ring across the P<sub>N</sub>-CO-Pro-NH-P<sub>C</sub> family. The simplest model is employed, with only two derived parameters, a puckering amplitude,  $A$ , which gives a maximum threshold to the five endocyclic  $\chi_i^j$  values,  $\chi_i^0, \chi_i^1, \chi_i^2, \chi_i^3$  and  $\chi_i^4$ , (illustrated in Figure 1b), whereas the phase angle,  $P$ , describes the state of pucker in the pseudorotation pathway, characterizing in some sense their ratios.

Using the algorithms described previously,<sup>43</sup> pseudorotational coordinates  $A$  and  $P$  were calculated from the values  $\chi_i^0, \chi_i^1, \chi_i^2, \chi_i^3$ , and  $\chi_i^4$ . The following three steps were taken to calculate  $A$  and  $P$  using the assumptions given in (5a) and (5b).

Taking into account that

$$\chi_i^0 = A \cos P \quad (5a)$$

and that

$$\sin^2 P + \cos^2 P = 1 \quad (5b)$$

then, as a First Step,

$$A \sin P = -(1/2)(\chi_i^1 - \chi_i^2 + \chi_i^3 - \chi_i^4)(\sin 144^\circ + \sin 72^\circ)^{-1} \quad (6)$$

as a Second Step,

$$A = [(A \sin P)^2 + (\chi_i^0)^2]^{1/2} \quad (7)$$

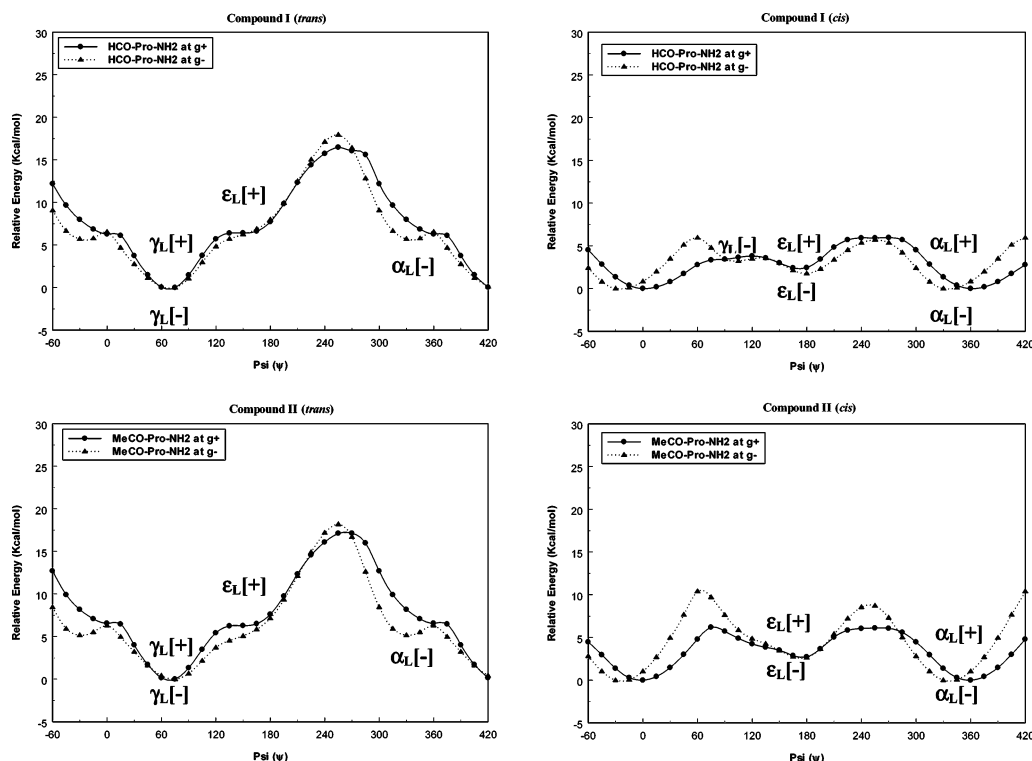


**Figure 6.** Potential energy curve (PEC)  $E = f(\psi_i)$  cross-sections of the conformational PES of compounds [I] and [II], showing both ring puckerings represented by syn ( $\chi_i^1 = g^+$ ) or DOWN (solid lines) and anti ( $\chi_i^1 = g^-$ ) or UP (broken lines).

**TABLE 2: Schematic Topological Pattern of Occurrence of Minimum Energy Conformers of Compounds [III] and [IV] at the RHF/3-21G Level of Theory**

SC	BB	trans-trans		trans-cis		cis-trans		cis-cis	
		III	IV	III	IV	III	IV	III	IV
$g^+$	$\alpha_L$		✓			✓	✓		✓
	$\epsilon_L$		✓			✓	✓		✓
	$\gamma_L$	✓	✓	✓	✓	✓	✓	✓	✓
$g^-$	$\alpha_L$	✓	✓	✓	✓	✓	✓	✓	✓
	$\epsilon_L$					✓	✓	✓	✓
	$\gamma_L$	✓	✓	✓	✓	✓	✓	✓	✓

and as a Third Step,

$$\text{If } A \sin P \geq 0, P = \cos^{-1}(\chi_i^0/A) \quad (8a)$$

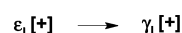
$$\text{If } A \sin P < 0, P = -\cos^{-1}(\chi_i^0/A) \quad (8b)$$

**2.3. Exploratory Computations.** **2.3.1. Geometry Optimizations.** In the first phase of the exploratory study, geometry optimizations were performed on all topologically possible MDCA-predicted conformers of HCO-Pro-NH<sub>2</sub> [I] at the RHF/3-21G level of theory.

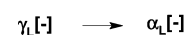
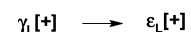
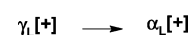
Geometry optimizations were performed in the same manner on the remaining amino acid diamide homologues, MeCO-Pro-NH<sub>2</sub> [II], HCO-Pro-NH-Me [III], and MeCO-Pro-NH-Me [IV], to determine the location of all minima on their respective conformational PEHS. Because only three backbone torsional angles ( $\gamma_L$ ,  $\epsilon_L$ ,  $\alpha_L$ ) and two ring puckerings, either syn ( $\chi_i^1 = g^+$ ) or “DOWN” or anti ( $\chi_i^1 = g^-$ ) or “UP”, are expected to exist, then,  $3 \times 2 = 6$  conformations are anticipated for each of the homologues. Regarding the  $\omega_i$  torsional angles, two isomers (trans and cis) may exist for compounds [I] and [II], which can lead to  $2 \times 2 = 4$  structures, whereas four isomers with trans-trans, trans-cis, cis-trans, and cis-cis

## SCHEME 2

$\omega_{i-1} = 180^\circ$   
isomers



$\omega_{i-1} = 0^\circ$   
isomers



peptide bonds for compounds [III] and [IV] result in  $4 \times 2 = 8$  structures for the  $\omega_{i-1}$  and  $\omega_i$  torsional angles. Therefore, a total of  $(4 + 8)6 = 72$  structures are predicted by MDCA to exist.

**2.3.2. Generation of Cross-Sections of Potential Energy Hypersurfaces (PEHS).** For compound [I], a PEHS (9) of the following form would have to be considered:

$$E = f^{\phi_i}(\omega_i, \psi_i, \chi_i^1) \quad (9)$$

where  $\phi_i$  is regarded as an optimized parameter.

A pair of relaxed cross-sections (10) and (11) with two independent variables corresponding to either preset but optimized  $\omega_i$ , or preset and optimized  $\chi_i^1$ , values were calculated for compound [I].

$$E = f^{\phi_i}_{\chi_i^1}(\chi_i^1, \psi_i) \quad (10)$$

$$E = f^{\phi_i}_{\omega_i}(\omega_i, \psi_i) \quad (11)$$

Four one-dimensional relaxed cross-sections (12), corresponding to initially preset but optimized  $\omega_i$  and  $\chi_i^1$  values, were computed

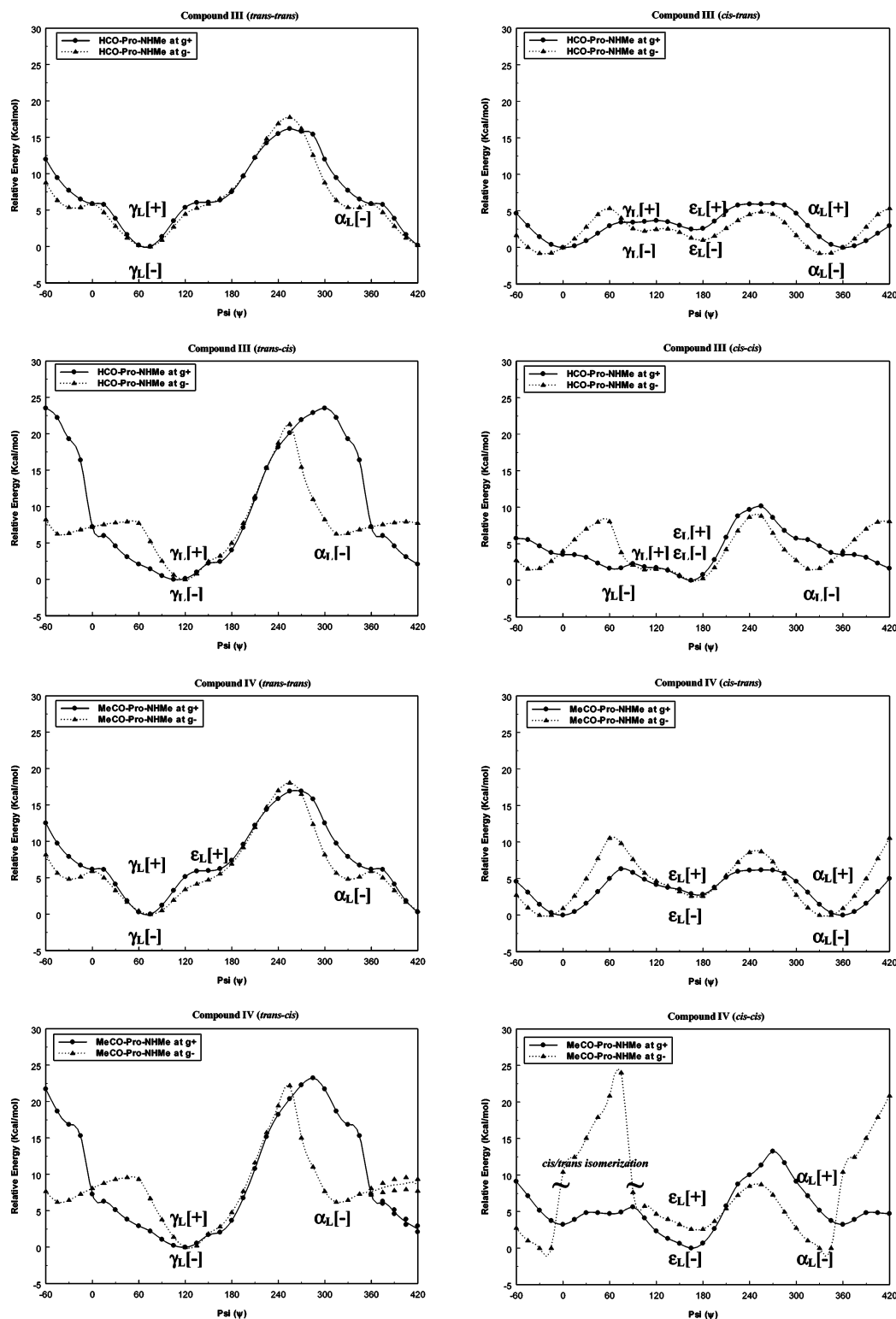


**Figure 7.** Potential energy curve (PEC)  $E = f(\psi)$  cross-sections of the conformational PES of compounds [III] and [IV], showing both ring puckerings represented by syn ( $\chi_i^1 = g^+$ ) or DOWN (solid lines) and anti ( $\chi_i^1 = g^-$ ) or UP (broken lines).

for compounds [I] and [III]. The preset values were  $\omega_{i-1} = 0^\circ$  (cis) and  $180^\circ$  (trans) as well as syn ( $\chi_i^1 = g^+$ ) or “DOWN” and anti ( $\chi_i^1 = g^-$ ) or “UP”.

$$E = f_{\omega, \chi_i^1}^{\phi_i}(\psi_i) \quad (12)$$

Eight one-dimensional relaxed cross-sections of the same type described in (12), corresponding to initially preset but optimized

$\omega_i$  and  $\chi_i^1$  values were also computed for compounds [III] and [IV]. The preset values were  $\omega_{i-1} = 0^\circ$  (cis) and  $180^\circ$  (trans) and  $\omega_i = 0^\circ$  (cis) and  $180^\circ$  (trans) as well as syn ( $\chi_i^1 = g^+$ ) or “DOWN” and anti ( $\chi_i^1 = g^-$ ) or “UP”.

All cross-sections of the PEHS were plotted.

**2.4. Detailed Computations.** Geometry optimizations were carried out at two further levels of theory, RHF/6-31G(d) and B3LYP/6-31G(d), on all four compounds [I]–[IV], allowing



for the assessment of the role of electron correlation, basis sets effects, as well as the relative importance of small and large N- and C-protecting groups.

**2.5. Advanced Computations.** Two composite methods, Complete Basis Set-4 Modified (CBS-4M)<sup>80–82</sup> and Gaussian-3 (G3MP2B3)<sup>83–85</sup> type procedures, were employed to generate accurate relative energies of compound [I], previously geometry-optimized at the RHF/3-21G and B3LYP/6-31G(d) levels of theory, respectively. The frequency calculation for both optimization levels confirmed that all stationary points selected were residing at minima on the PEHS.

### 3. Results and Discussion

**3.1. Exploratory Computations.** A pair of cross-sections with two independent variables of the type (10) and (11) were generated at the RHF/3-21G level of theory to present an initial first-prediction of the conformations that may reside at minima on the PEHS of type (9). These PESs are presented in Figures 4 and 5. On each of the pairs of  $E = f(\chi_i^1, \psi_i)$  PESs (Figure 4) associated with the trans and cis peptide bonds, along each of the two lines  $\chi_i^1 = g^+$  and  $\chi_i^1 = g^-$ , three minima ( $\gamma_L$ ,  $\epsilon_L$ , and  $\alpha_L$ ) are expected. Similarly, on each of the pairs of  $E = f(\omega_i, \psi_i)$  PESs (Figure 5) associated with  $\chi_i^1 = g^+$  and  $\chi_i^1 = g^-$  ring puckering, along the two lines  $\omega_{i-1} = 0^\circ$  (cis) and  $\omega_i = 180^\circ$  (trans), three minima ( $\gamma_L$ ,  $\epsilon_L$ , and  $\alpha_L$ ) are also expected. A number of the expected six minima for each of the two surfaces presented in Figures 4 and 5 were annihilated.

Although the relative stabilities of local minima for the four compounds, [I]–[IV], differ from each other, there are no significant differences in the overall PESs as indicated in Figure 4 for  $E = f(\chi_i^1, \psi_i)$  and Figure 5 for  $E = f(\omega_i, \psi_i)$ . Even though compound [I] was used to generate these PESs at the RHF/3-21G level of theory, these results are similar to previous studies done on compound [IV] utilizing various methods and basis sets.<sup>34,38,41,48</sup>

For further details, cross-sections of a single independent variable of type (12) were computed for compound [I]. The four curves, trans [ $\chi_i^1 = g^+$ ] and trans [ $\chi_i^1 = g^-$ ] as well as cis [ $\chi_i^1 = g^+$ ] and cis [ $\chi_i^1 = g^-$ ], are depicted graphically in the upper portion of Figure 6. Two observations may be made at this point.

The two trans PEC are very similar in shape, and the two cis PEC also portrayed a similar shape. On the other hand, the pair of trans PEC is quite different from the two cis PEC. The energy barriers of the cis PEC are only about half as high as those of the trans PEC from the baseline. This means that energetically, the cis proline residue is considerably more flexible than the trans proline residue. In fact, the trans residue is quite rigid with respect to the cis residue.

Similarly, four PEC were generated for compound [III]. The results obtained from compound [III] are remarkably similar to the results generated for compound [I]. These are shown at the lower part of Figure 6, whereas those of compound [I] are presented in the upper part of Figure 6 for the sake of comparison. A schematic topology of the occurrence of the minima ( $\gamma_L$ ,  $\epsilon_L$ , and  $\alpha_L$ ) associated with compounds [I] and [III] is shown in Table 1.

Compounds [III] and [IV] were also subjected to an analogous study and the PEC are shown in Figure 7. It should be noted that the cis–cis isomer of MeCO–Pro–NH–Me [IV] showed cis–trans isomerization with respect to  $\omega_{i-1}$ , at  $\psi_i$  values from  $0^\circ$  to  $105^\circ$ , although it would be necessary to perform dynamic simulations to confirm the results seen in Figure 7. The topology of the occurrence of the minima ( $\gamma_L$ ,  $\epsilon_L$ , and  $\alpha_L$ ) is shown in Table 2 for compounds [III] and [IV].

In conjunction with Figure 3, Table 3 illustrates the geometrical and energetic characteristics of HCO–Pro–NH<sub>2</sub> [I], HCO–Pro–NH–Me [II], MeCO–Pro–NH<sub>2</sub> [III], and MeCO–Pro–NH–Me [IV] computed at the RHF/3-21G level of theory. The calculated *A* and *P* values are also included in Table 3. A total of 50 conformers out of the 72 topologically possible structures were located. The remaining  $(72 - 50) = 22$  structures migrated to the corresponding minima as illustrated in Scheme 2.

One exception was also noted in the case of the cis–cis isomer of compound [III] where the shift took place from  $\alpha_L$ –[+] to  $\gamma_L$ –[+], which was distorted toward a  $\delta_L$ –[+] conformation (just outside the normal  $\phi_i$  value). This distortion happened despite the fact that the  $\delta_L$  conformation normally does not exist in the case of proline.<sup>35</sup> The  $\phi_i$  and  $\psi_i$  values were  $-121.65^\circ$  and  $+66.71^\circ$ , respectively, as listed in Table 3 under  $\gamma_L$ –[+]\* for HCO–Pro–NH–Me [III]. This indicates the possibility of a  $\delta_L$  conformation existing for proline, using electronic structure methods, although it has been found from a search of 1135 nonhomogeneous proteins in the Brookhaven PDB.<sup>35</sup>

The global minima for compounds [I] and [II] was found to be trans- $\gamma_L$ –[+]; for compounds [III] and [IV] it was also  $\gamma_L$ –[+], but in the trans–trans isomer. For compounds [I] and [II], the local minimum was at the cis- $\alpha_L$ –[+] conformation. Likewise, for the cis–trans isomers of compounds [III] and [IV], the  $\alpha_L$ –[+] conformer was at the lowest energy values. However, for the cis–cis isomers of compounds [III] and [IV], the  $\epsilon_L$ –[+] conformer was found to be the local minima. Additionally, for the trans–cis and trans–trans isomers of compounds [III] and [IV], the local minima were at the  $\gamma_L$ –[+] conformation. Clearly, the orientation of both peptide bonds determines the stability of the eventual structure.

**3.2. Detailed Computations.** Increasing the basis set size on theoretical refinement from RHF/3-21G to RHF/6-31G(d) resulted in the disappearance of some minima. This is seen through comparisons of the data presented in Tables 3 and 4. Unlike the 50 conformers found at the RHF/3-21G level of theory, only 41 out of the 72 topologically possible structures were located at the RHF/6-31G(d) level of theory. The remaining  $(72 - 41) = 31$  structures migrated to minima corresponding to minima, as illustrated in Scheme 2, in addition to  $\alpha_L$ –[–] conformers migrating to  $\gamma_L$ –[–] for  $\omega_{i-1} = 180^\circ$  and  $\omega_i = 180^\circ$ , corresponding to trans–trans isomers. The PEHS becomes smoother and the relatively shallow RHF/3-21G minima become inflection points on the RHF/6-31G(d) PEHS.

Disappearance as well as appearance and reappearance of minima occurred at the B3LYP/6-31G(d) level of theory. The results are summarized in Table 5. Similarly to RHF/6-31G(d), 41 conformers were found at the B3LYP/6-31G(d) level of theory with the same migration pattern.

It would now be important to consider a comparison of the existing minima found at the three levels of theory. For illustrative purposes, a comparison of the existing minima found at the three levels of theory is shown in Table 6, whereas a schematic depiction is given in Figure 8. It should be noted that the distribution of local minima at RHF/3-21G is different from those at the RHF/6-31G(d) and B3LYP/6-31G(d) levels of theory.

However, it would be necessary to assess the role of electron correlation, basis sets effects, as well as the relative importance of the use of small and large N- and C-protecting groups.

First, for an overall correlation, the relative energies listed in Tables 3–5 are plotted in Figure 9. As is seen in Figure 9, the increased basis set size reduced the  $\Delta E$  values, measured

isomer	conformer BB [SC]	energy				dihedral angles										pseudorotation parameters	
		relative (kcal·mol <sup>-1</sup> )														A <sup>b</sup>	P
		total (Hartrees)	ΔE <sub>GL</sub>	ΔE <sub>LO</sub>	ψ <sub>i-1</sub>	ω <sub>i-1</sub>	φ <sub>i</sub>	ψ <sub>i</sub>	ω <sub>i</sub>	φ <sub>i+1</sub>	χ <sub>i</sub> <sup>0</sup>	χ <sub>i</sub> <sup>1</sup>	χ <sub>i</sub> <sup>2</sup>	χ <sub>i</sub> <sup>3</sup>	χ <sub>i</sub> <sup>4</sup>		
HCO-Pro-NH <sub>2</sub> [Compound I]																	
c	α <sub>L</sub> [+]	-488.945374	5.63	0.00		10.30	-96.60	2.09	-0.64		-17.21	34.56	-39.61	29.15	-7.50	39.91	115.55
	α <sub>L</sub> [-]	-488.943170	7.01	1.38		9.33	-67.47	-26.14	4.76		9.98	-30.03	39.01	-32.33	14.15	38.84	-75.11
	ε <sub>L</sub> [+]	-488.941638	7.98	2.34		-7.70	-62.43	172.35	-3.32		-13.42	32.75	-40.22	31.83	-11.64	40.14	109.53
	ε <sub>L</sub> [-]	-488.940219	8.87	3.23		-3.77	-51.10	178.50	-0.96		6.21	-27.42	38.18	-33.79	17.54	38.50	-80.72
	γ <sub>L</sub> [+]						not found – migrated to α <sub>L</sub> [+]										
t	γ <sub>L</sub> [-]	-488.937926	10.30	4.67		1.80	-59.15	101.39	4.66		4.88	-26.49	38.06	-34.11	18.65	38.43	82.70
	α <sub>L</sub> [+]						not found – migrated to γ <sub>L</sub> [+]										
	α <sub>L</sub> [-]	-488.941002	8.37	8.37		-171.42	-74.41	-23.50	10.14		4.62	-26.80	38.49	-34.99	19.32	39.13	83.22
	ε <sub>L</sub> [+]	-488.943850	6.59	6.59		175.82	-70.97	150.61	-12.83		-15.47	33.62	-39.78	30.18	-9.29	39.80	-112.87
	ε <sub>L</sub> [-]						not found – migrated to γ <sub>L</sub> [-]										
	γ <sub>L</sub> [+]	-488.954348	0.00	0.00		-173.03	-83.32	67.91	-4.13		-15.18	33.49	-39.99	30.32	-9.61	39.85	-112.39
	γ <sub>L</sub> [-]	-488.951950	1.50	1.50		-171.87	-82.66	68.69	-5.36		-12.75	-11.63	30.27	-37.02	31.71	38.14	109.53
MeCO-Pro-NH <sub>2</sub> [Compound II]																	
c	α <sub>L</sub> [+]	-527.775130	5.49	0.00	171.03	10.65	-90.35	-1.95	-2.00		-13.86	32.98	-40.04	31.46	-11.08	40.02	-110.26
	α <sub>L</sub> [-]	-527.772518	7.13	1.64	179.04	9.50	-74.30	-23.67	4.64		5.37	-27.24	38.59	-34.75	18.63	39.10	82.11
	ε <sub>L</sub> [+]	-527.770883	8.16	2.67	-174.11	-2.60	-70.87	174.70	-2.30		-15.75	34.18	-40.25	30.61	-9.33	40.36	-112.97
	ε <sub>L</sub> [-]	-527.768549	9.62	4.13	-169.74	-3.51	-65.28	178.08	-0.68		-4.29	-19.89	35.60	-37.43	26.63	39.08	96.30
	γ <sub>L</sub> [+]						not found – migrated to α <sub>L</sub> [+]										
t	γ <sub>L</sub> [-]						not found – migrated to α <sub>L</sub> [-] or ε <sub>L</sub> [-]										
	α <sub>L</sub> [+]						not found – migrated to γ <sub>L</sub> [+]										
	α <sub>L</sub> [-]	-52															

TABLE 3: (Continued)

isomer	conformer BB [SC]	energy				dihedral angles										pseudorotation parameters	
		total (Hartrees)	relative (kcal·mol <sup>-1</sup> )		$\psi_{i-1}$	$\omega_{i-1}$	$\phi_i$	$\psi_i$	$\omega_i$	$\phi_{i+1}$	$\chi_i^0$	$\chi_i^1$	$\chi_i^2$	$\chi_i^3$	$\chi_i^4$	$A^b$	$P$
			$\Delta E_{\text{GL}}$	$\Delta E_{\text{LO}}$													
HCO-Pro-NH-Me [Compound III] (Continued)																	
	$\epsilon_{\text{L}}[-]$				not found – migrated to $\gamma_{\text{L}}[-]$												
	$\gamma_{\text{L}}[+]$	-527.768256	0.00	0.00	-173.08	-83.71	68.84	-178.90	112.88	-15.56	33.69	-40.00	30.08	-9.21	39.87	-112.97	
	$\gamma_{\text{L}}[-]$	-527.765765	1.56	1.56	-172.01	-82.60	69.89	-178.97	-167.63	-12.73	-11.65	30.28	-37.01	31.69	38.13	109.50	
MeCO-Pro-NH-Me [Compound IV]																	
cc	$\alpha_{\text{L}}[+]$	-566.573533	15.21	3.21	171.74	6.38	-83.09	-5.54	-8.64	-166.84	-13.34	32.04	-38.97	30.67	-10.93	38.95	-110.03
	$\alpha_{\text{L}}[-]$	-566.574132	14.83	2.84	-172.47	6.72	-62.22	-37.02	-0.05	-164.77	8.81	-28.92	38.16	-32.42	14.93	38.21	76.67
	$\epsilon_{\text{L}}[+]$	-566.578656	11.99	0.00	-173.53	-2.50	-70.31	167.49	-9.62	178.00	-14.79	33.73	-40.51	31.37	-10.40	40.49	-111.42
	$\epsilon_{\text{L}}[-]$	-566.575777	13.80	1.81	-166.19	-4.09	-61.64	167.58	-7.60	-179.03	-2.39	-21.41	36.38	-37.02	25.15	39.05	-93.51
	$\gamma_{\text{L}}[+]$																
ct	$\gamma_{\text{L}}[-]$																
	$\alpha_{\text{L}}[+]$	-566.589742	5.04	0.00	170.59	10.81	-90.83	-1.58	-178.89	116.19	-14.15	33.19	-40.13	31.37	-10.85	40.12	-110.65
	$\alpha_{\text{L}}[-]$	-566.586932	6.80	1.76	177.95	9.20	-75.12	-22.27	-175.48	116.02	4.46	-26.61	38.40	-35.08	19.43	39.09	83.45
	$\epsilon_{\text{L}}[+]$	-566.585367	7.78	2.75	-173.89	-2.86	-70.35	174.08	179.00	119.72	-15.81	34.30	-40.40	30.71	-9.36	40.50	-112.98
	$\epsilon_{\text{L}}[-]$	-566.583009	9.26	4.23	-169.42	-3.93	-65.00	176.73	178.72	120.64	-3.77	-20.32	35.82	-37.32	26.24	39.08	95.54
tc	$\gamma_{\text{L}}[+]$																
	$\gamma_{\text{L}}[-]$																
	$\alpha_{\text{L}}[+]$																
	$\alpha_{\text{L}}[-]$	-566.571548	16.45	8.56	-171.87	-175.79	-55.82	-41.04	9.30	-165.86	11.22	-30.50	38.34	-31.19	12.61	38.28	-72.96
	$\epsilon_{\text{L}}[+]$																
tt	$\epsilon_{\text{L}}[-]$																
	$\gamma_{\text{L}}[+]$	-566.585190	7.89	0.00	178.62	-178.99	-84.17	117.56	-9.01	-163.03	-17.59	33.39	-37.40	26.47	-5.58	37.76	-117.76
	$\gamma_{\text{L}}[-]$	-566.582558	9.55	1.65	-176.80	-179.89	-89.58	111.49	-3.24	-164.25	-23.51	-2.00	24.81	-38.15	39.26	41.22	-124.77
	$\alpha_{\text{L}}[+]$	-566.587879	6.21	6.21	-175.07	-171.87	-97.04	7.85	177.46	123.43	-17.96	35.54	-40.29	29.48	-7.28	40.75	116.15
	$\alpha_{\text{L}}[-]$	-566.583983	8.65	8.65	-169.55	-175.46	-67.17	-28.80	-178.79	125.66	8.47	-29.02	38.60	-32.91	15.47	38.63	77.33
	$\epsilon_{\text{L}}[+]$	-566.588094	6.07	6.07	172.62	176.82	-72.09	147.55	178.28	110.34	-16.84	34.06	-39.12	28.82	-7.55	39.38	115.32
	$\epsilon_{\text{L}}[-]$																
	$\gamma_{\text{L}}[+]$	-566.597769	0.00	0.00	178.68	-173.34	-85.28	69.95	-178.91	113.00	-16.81	34.43	-39.88	29.38	-7.97	39.99	114.86
	$\gamma_{\text{L}}[-]$	-566.593778	2.50	2.50	-175.56	-175.15	-83.04	72.55	-178.81	-165.92	-15.08	-9.40	28.91	-37.24	33.21	38.42	113.11

<sup>a</sup> Asterisk indicates distortion toward  $\delta_L[+]$ . <sup>b</sup> Average A value = 39.25.



TABLE 4: (Continued)

isomer	conformer BB [SC]	energy			dihedral angles											pseudorotation parameters				
		total (Hartrees)	relative (kcal·mol <sup>-1</sup> )		$\psi_{i-1}$	$\omega_{i-1}$	$\phi_i$	$\psi_i$	$\omega_i$	$\phi_{i+1}$	$\chi_i^0$	$\chi_i^1$	$\chi_i^2$	$\chi_i^3$	$\chi_i^4$	$A^a$	$P$			
MeCO–Pro–NH–Me [Compound IV] (Cont'd)																				
	$\gamma_L[+]$	−530.719582	0.00	0.00	−172.15	−85.36	73.40	−175.72	67.54	−13.93	31.50	−37.84	28.93	−9.46	37.67	−111.70				
	$\gamma_L[-]$	−530.717938	1.03	1.03	−170.36	−84.64	78.02	−174.52	−172.31	−9.29	−14.94	32.32	−37.18	29.61	38.20	−104.07				
MeCO–Pro–NH–Me [Compound IV]																				
cc	$\alpha_L[+]$	−569.744771	11.38	2.51	169.85	7.91	−83.62	−12.80	−4.40	−169.05	−12.32	30.01	−36.65	28.92	−10.45	36.59	109.68			
	$\alpha_L[-]$	−569.745760	10.76	1.89	72.96	6.28	−63.66	−38.04	−0.24	−164.86	7.67	−27.53	36.97	−32.03	15.36	37.16	78.09			
	$\epsilon_L[+]$	−569.748771	8.87	0.00	−175.24	−3.56	−72.46	163.90	−12.00	56.52	−18.63	33.66	−36.81	25.62	−4.26	37.55	119.74			
	$\epsilon_L[-]$	−569.747030	9.96	1.09	−158.17	−5.76	−58.69	158.45	−8.72	174.89	−2.03	−20.94	35.27	−35.86	24.12	37.81	−93.08			
	$\gamma_L[+]$							not found	− migrated to $\epsilon_L[+]$											
ct	$\gamma_L[-]$							not found	− migrated to $\epsilon_L[-]$											
	$\alpha_L[+]$	−569.758087	3.02	0.00	168.15	10.72	−90.66	−5.54	−178.05	−172.68	−13.36	31.51	−38.13	29.82	−10.34	38.10	−110.53			
	$\alpha_L[-]$	−569.756175	4.22	1.20	176.17	7.29	−76.43	−21.60	−175.69	64.79	2.48	−24.36	36.61	−34.64	20.35	37.76	−86.23			
	$\epsilon_L[+]$	−569.753973	5.61	2.58	−175.82	−3.41	−71.82	159.69	174.11	166.02	−18.09	33.52	−37.01	26.09	−4.93	37.63	−118.73			
	$\epsilon_L[-]$	−569.752692	6.41	3.39	−157.95	−4.60	−57.30	155.63	178.19	−167.86	0.57	−22.96	36.09	−35.16	22.00	37.76	89.14			
tc	$\gamma_L[+]$							not found	− migrated to $\epsilon_L[+]$											
	$\gamma_L[-]$							not found	− migrated to $\epsilon_L[-]$											
	$\alpha_L[+]$							not found	− migrated to $\epsilon_L[+]$											
	$\alpha_L[-]$	−569.744987	11.24	5.67	−168.14	−172.94	−59.68	−38.07	16.27	70.70	−14.95	−29.88	30.54	−35.16	−6.90	32.46	−117.42			
	$\epsilon_L[+]$	−569.754027	5.57	0.00	169.76	177.38	−69.19	138.04	−22.30	−168.83	−14.68	30.35	−35.12	26.05	−7.14	35.26	114.60			
tt	$\epsilon_L[-]$	−569.752825	6.33	0.75	−176.69	175.41	−59.85	135.51	−23.02	−169.47	−5.44	−18.17	33.98	−36.48	26.68	37.86	−98.26			
	$\gamma_L[+]$							not found	− migrated to $\epsilon_L[+]$											
	$\gamma_L[-]$							not found	− migrated to $\epsilon_L[-]$											
	$\alpha_L[+]$							not found	− migrated to $\gamma_L[+]$											
	$\alpha_L[-]$	−569.755977	4.35	4.35	−165.98	−171.28	−70.98	−20.93	175.42	169.26	6.50	−27.32	37.63	−33.32	16.92	37.99	−80.15			
	$\epsilon_L[+]$							not found	− migrated to $\gamma_L[+]$											
	$\epsilon_L[-]$							not found	− migrated to $\gamma_L[-]$											
	$\gamma_L[+]$	−569.762907	0.00	0.00	−178.64	−172.94	−86.08	75.83	−175.57	67.50	−14.71	32.07	−37.87	28.63	−8.77	37.85	−112.87			
	$\gamma_L[-]$	−569.759833	1.93	1.93	−169.54	−175.15	−82.11	85.57	−173.74	−171.91	−10.42	−13.70	31.44	−37.11	30.18	37.99	−105.92			

<sup>a</sup> Average A value = 37.46.





TABLE 5: (Continued)

isomer	conformer BB [SC]	energy			dihedral angles										pseudorotation parameters				
		total (Hartrees)	relative (kcal·mol <sup>-1</sup> )		$\psi_{i-1}$	$\omega_{i-1}$	$\phi_i$	$\psi_i$	$\omega_i$	$\phi_{i+1}$	$\chi_i^0$	$\chi_i^1$	$\chi_i^2$	$\chi_i^3$	$\chi_i^4$	$A^a$	$P$		
			$\Delta E_{GL}$	$\Delta E_{LO}$															
HCO-Pro-NH-Me [Compound III] (Continued)																			
	$\epsilon_L[-]$				not found – migrated to $\gamma_L[-]$														
	$\gamma_L[+]$	-533.949884	0.00	0.00	-172.23	-82.37	68.65	-177.54	107.40	-13.13	31.26	-38.27	29.79	-10.50	38.02	-110.20			
	$\gamma_L[-]$	-533.949450	0.27	0.27	-169.98	-82.46	71.97	-176.40	99.34	-9.57	-14.14	31.36	-36.35	29.24	37.34	-104.85			
MeCO-Pro-NH-Me [Compound IV]																			
cc	$\alpha_L[+]$	-573.252805	12.19	1.93	172.15	5.15	-80.85	-11.89	-6.73	-168.13	-13.31	30.55	-36.67	28.36	-9.44	36.70	-111.26		
	$\alpha_L[-]$	-573.253908	11.49	1.24	74.55	5.91	-62.39	-39.97	2.11	-47.99	7.05	-27.19	37.05	-33.02	15.99	37.27	-79.10		
	$\epsilon_L[+]$	-573.255887	10.25	0.00	-173.83	-2.75	-71.19	162.43	-6.68	47.42	-17.03	33.23	-37.60	27.30	-6.34	37.98	-116.64		
	$\epsilon_L[-]$	-573.254741	10.97	0.72	-163.36	-0.44	-61.50	157.05	-7.34	171.88	0.48	-22.71	35.81	-34.96	21.91	37.50	89.27		
	$\gamma_L[+]$				not found – migrated to $\epsilon_L[+]$														
ct	$\gamma_L[-]$				not found – migrated to $\epsilon_L[-]$														
	$\alpha_L[+]$	-573.265312	4.34	0.00	168.41	11.47	-92.75	-2.17	-179.22	115.69	-14.07	31.83	-38.02	29.32	-9.55	38.02	-111.72		
	$\alpha_L[-]$	-573.263650	5.38	1.04	175.36	11.13	-78.81	-19.00	-176.36	-0.23	2.77	-24.53	36.68	-34.55	20.07	37.74	-85.79		
	$\epsilon_L[+]$	-573.260874	7.12	2.78	-178.66	-2.22	-73.98	143.57	175.64	122.02	-16.32	32.38	-36.87	26.89	-6.57	37.15	116.06		
	$\epsilon_L[-]$	-573.260096	7.61	3.27	-164.93	-1.19	-57.74	146.76	176.84	114.93	3.59	-25.08	36.75	-34.02	19.33	37.60	84.52		
tc	$\gamma_L[+]$				not found – migrated to $\epsilon_L[+]$														
	$\gamma_L[-]$				not found – migrated to $\epsilon_L[-]$														
	$\alpha_L[+]$				not found – migrated to $\epsilon_L[+]$														
	$\alpha_L[-]$	-573.252446	12.41	5.67	-169.89	-173.15	-57.69	-39.04	18.64	-170.61	9.68	-29.22	37.84	-31.58	13.80	37.79	-75.16		
	$\epsilon_L[+]$	-573.261488	6.74	0.00	173.24	-179.49	-77.54	123.53	-14.75	-161.46	-14.53	30.88	-36.15	27.05	-7.84	36.16	113.69		
tt	$\epsilon_L[-]$	-573.260569	7.31	0.58	-176.09	177.17	-62.09	127.57	-20.36	-165.16	-3.37	-19.97	34.99	-36.24	25.21	37.97	95.09		
	$\gamma_L[+]$				not found – migrated to $\epsilon_L[+]$														
	$\gamma_L[-]$				not found – migrated to $\epsilon_L[-]$														
	$\alpha_L[+]$				not found – migrated to $\gamma_L[+]$														
	$\alpha_L[-]$	-573.262360	6.19	6.19	-166.44	-171.08	-74.51	-16.17	176.82	138.25	3.90	-25.38	36.93	-34.14	19.09	37.74	84.07		
	$\epsilon_L[+]$				not found – migrated to $\gamma_L[+]$														
	$\epsilon_L[-]$				not found – migrated to $\gamma_L[-]$														
	$\gamma_L[+]$	-573.272224	0.00	0.00	179.31	-172.31	-83.96	70.85	-176.99	108.15	-13.99	31.77	-38.15	29.31	-9.66	38.05	-111.57		
	$\gamma_L[-]$	-573.270265	1.23	1.23	-172.91	-173.04	-82.26	76.68	-175.48	95.13	-10.64	-13.18	30.84	-36.65	30.00	37.50	-106.48		

<sup>a</sup> Average A value = 37.56.

**TABLE 6: Occurrences of Optimized Minima of Compounds [I]–[IV] at Three Levels of Theory**

compd	isomer	conformer	occurrence of minima		
			RHF/3-21G	RHF/6-31G(d)	B3LYP/6-31G(d)
I	c	$\alpha_L[+]$	✓	✓	✓
		$\alpha_L[-]$	✓	✓	✓
		$\epsilon_L[+]$	✓	✓	✓
		$\epsilon_L[-]$	✓	✓	✓
		$\gamma_L[+]$			
		$\gamma_L[-]$	✓		
	t	$\alpha_L[+]$			
		$\alpha_L[-]$	✓		
		$\epsilon_L[+]$	✓		
		$\epsilon_L[-]$			
		$\gamma_L[+]$	✓	✓	✓
		$\gamma_L[-]$	✓	✓	✓
II	c	$\alpha_L[+]$	✓	✓	✓
		$\alpha_L[-]$	✓	✓	✓
		$\epsilon_L[+]$	✓	✓	✓
		$\epsilon_L[-]$	✓	✓	✓
		$\gamma_L[+]$	✓	✓	✓
		$\gamma_L[-]$	✓	✓	✓
	t	$\alpha_L[+]$			
		$\alpha_L[-]$	✓	✓	
		$\epsilon_L[+]$	✓		
		$\epsilon_L[-]$			
		$\gamma_L[+]$	✓	✓	✓
		$\gamma_L[-]$	✓	✓	✓
III	cc	$\alpha_L[+]$	✓	✓	✓
		$\alpha_L[-]$	✓	✓	✓
		$\epsilon_L[+]$	✓	✓	✓
		$\epsilon_L[-]$	✓	✓	✓
		$\gamma_L[+]$	✓	✓	✓
		$\gamma_L[-]$	✓	✓	✓
	ct	$\alpha_L[+]$	✓	✓	✓
		$\alpha_L[-]$	✓	✓	✓
		$\epsilon_L[+]$	✓	✓	✓
		$\epsilon_L[-]$	✓	✓	✓
		$\gamma_L[+]$	✓	✓	✓
		$\gamma_L[-]$	✓	✓	✓
	tc	$\alpha_L[+]$	✓	✓	✓
		$\alpha_L[-]$	✓	✓	✓
		$\epsilon_L[+]$	✓	✓	✓
		$\epsilon_L[-]$	✓	✓	✓
		$\gamma_L[+]$	✓	✓	✓
		$\gamma_L[-]$	✓	✓	✓
	tt	$\alpha_L[+]$	✓	✓	✓
		$\alpha_L[-]$	✓	✓	✓
		$\epsilon_L[+]$	✓	✓	✓
		$\epsilon_L[-]$	✓	✓	✓
		$\gamma_L[+]$	✓	✓	✓
		$\gamma_L[-]$	✓	✓	✓
IV	cc	$\alpha_L[+]$	✓	✓	✓
		$\alpha_L[-]$	✓	✓	✓
		$\epsilon_L[+]$	✓	✓	✓
		$\epsilon_L[-]$	✓	✓	✓
		$\gamma_L[+]$	✓	✓	✓
		$\gamma_L[-]$	✓	✓	✓
	ct	$\alpha_L[+]$	✓	✓	✓
		$\alpha_L[-]$	✓	✓	✓
		$\epsilon_L[+]$	✓	✓	✓
		$\epsilon_L[-]$	✓	✓	✓
		$\gamma_L[+]$	✓	✓	✓
		$\gamma_L[-]$	✓	✓	✓
	tc	$\alpha_L[+]$	✓	✓	✓
		$\alpha_L[-]$	✓	✓	✓
		$\epsilon_L[+]$	✓	✓	✓
		$\epsilon_L[-]$	✓	✓	✓
		$\gamma_L[+]$	✓	✓	✓
		$\gamma_L[-]$	✓	✓	✓
	tt	$\alpha_L[+]$	✓	✓	✓
		$\alpha_L[-]$	✓	✓	✓
		$\epsilon_L[+]$	✓	✓	✓
		$\epsilon_L[-]$	✓	✓	✓
		$\gamma_L[+]$	✓	✓	✓
		$\gamma_L[-]$	✓	✓	✓

with respect to the global minima, whereas the subsequent electron correlation substantially increased  $\Delta E$  back toward values obtained at the RHF/3-21G level of theory.

Further correlations for torsional angles ( $\omega_{i-1}$ ,  $\phi_i$ ,  $\psi_i$ , and  $\chi_i^1$ ) were made across the three levels of theory. This is illustrated in Figure 10.

From Figure 10, very good correlations exist for the torsional angles ( $\omega_{i-1}$ ,  $\phi_i$ ,  $\psi_i$ , and  $\chi_i^1$ ) across the three levels of theory. Because  $R^2 \approx 0.9$ , this indicates that the torsional angles obtained are quite similar irrespective of the level of theory at which the simulations were performed (RHF/3-21G, RHF/6-31G(d) and B3LYP/6-31G(d)) for the four compounds, [I]–[IV].

These results as well as those from Figure 9 are quite significant, as they indicate the reliability of a small basis set (i.e., RHF/3-21G) in giving a faithful representation of electron distribution that would be similarly found with a higher basis set (i.e., RHF/6-31G(d) or B3LYP/6-31G(d)). Also, one can see that using  $P_N = P_C = H$ , similar to compound [I], is not a misleading practice in analyzing peptide models as minor differences in geometry are observed when either  $P_N$  or  $P_C$  or both are  $CH_3$  groups rather than H. Therefore, RHF/3-21G computations as well as the use of the simplest model, compound [I] with  $P_N = P_C = H$ , give reasonable first approximations to both geometry and stability with no cost of time and the additional computational power, as was found in a previous study.<sup>54</sup>

Distinguishing cis from trans type conformers and  $\chi_i^1 = g^+$  from  $\chi_i^1 = g^-$  ring puckers from the optimized dihedral angles was trivial. However, it is important to note that when distinguishing the backbone conformers of  $\gamma_L$ ,  $\epsilon_L$ , and  $\alpha_L$ , the ideally expected threshold values of  $\psi_i = 0^\circ$  and  $120^\circ$  proved to be unacceptable as the  $\psi_i$  values of  $\epsilon_L$  type conformers were found to be as low as  $118.77^\circ$  rather than the ideal value of  $180^\circ$ , whereas that of  $\alpha_L$  type conformers were found to be as high as  $7.85^\circ$  instead of the ideal value of  $-60^\circ$ . This is in agreement with established deviations.<sup>39</sup>

Consideration of the PES along the backbone torsion angle  $\psi_i$  also shows that within each compound, [I]–[IV], there are certain general trends relating to found conformers residing at minima. Across the three levels of theory and the four compounds, the “DOWN” puckering stabilizes values of  $\psi$  close to  $+160^\circ$  ( $\epsilon_L$  minima) or  $-20^\circ$  ( $\alpha_L$  minima), whereas “UP” puckering stabilizes values of  $\psi$  close to  $+160^\circ$  ( $\epsilon_L$  minima) and  $-3^\circ$  ( $\alpha_L$  minima). These findings are in accordance with previous results, where the HF/6-31G(d) and the HF/6-31+G-(d) levels of theory were used for the trans proline dipeptide<sup>38</sup> and the trans and cis MeCO–Pro–NH–Me,<sup>48</sup> respectively. Overall, all ideal  $\epsilon_L$  and  $\alpha_L$  type conformers are present for the four compounds, [I]–[IV], but negative ring puckers following cis peptide bonds are rare, as shown previously.<sup>39</sup>

The ring puckering parameters  $A$  and  $P$  were calculated at all three levels of theory, as summarized in Tables 3–5. The functional dependence of  $\chi_i^0$  in terms of  $P$  using the average  $\bar{A}$  value, as shown in (13), is analogous to that of (5a)

$$\chi_i^0 = \bar{A} \cos P \quad (13)$$

The functional variation of  $\chi_i^0$ ,  $\chi_i^1$ ,  $\chi_i^2$ ,  $\chi_i^3$ , and  $\chi_i^4$  with  $P$  is shown in the upper part of Figure 11 and illustrates how the five parameters  $\chi_i^0$ ,  $\chi_i^1$ ,  $\chi_i^2$ ,  $\chi_i^3$ , and  $\chi_i^4$  can be reduced to two parameters  $A$  and  $P$ . The change of  $\chi_i^0$  with  $P$  at the RHF/3-21G level of theory is illustrated at the bottom of Figure 11. The average  $\bar{A}$  value was found to be  $39.25^\circ$ , as listed in the footnotes of Table 3.

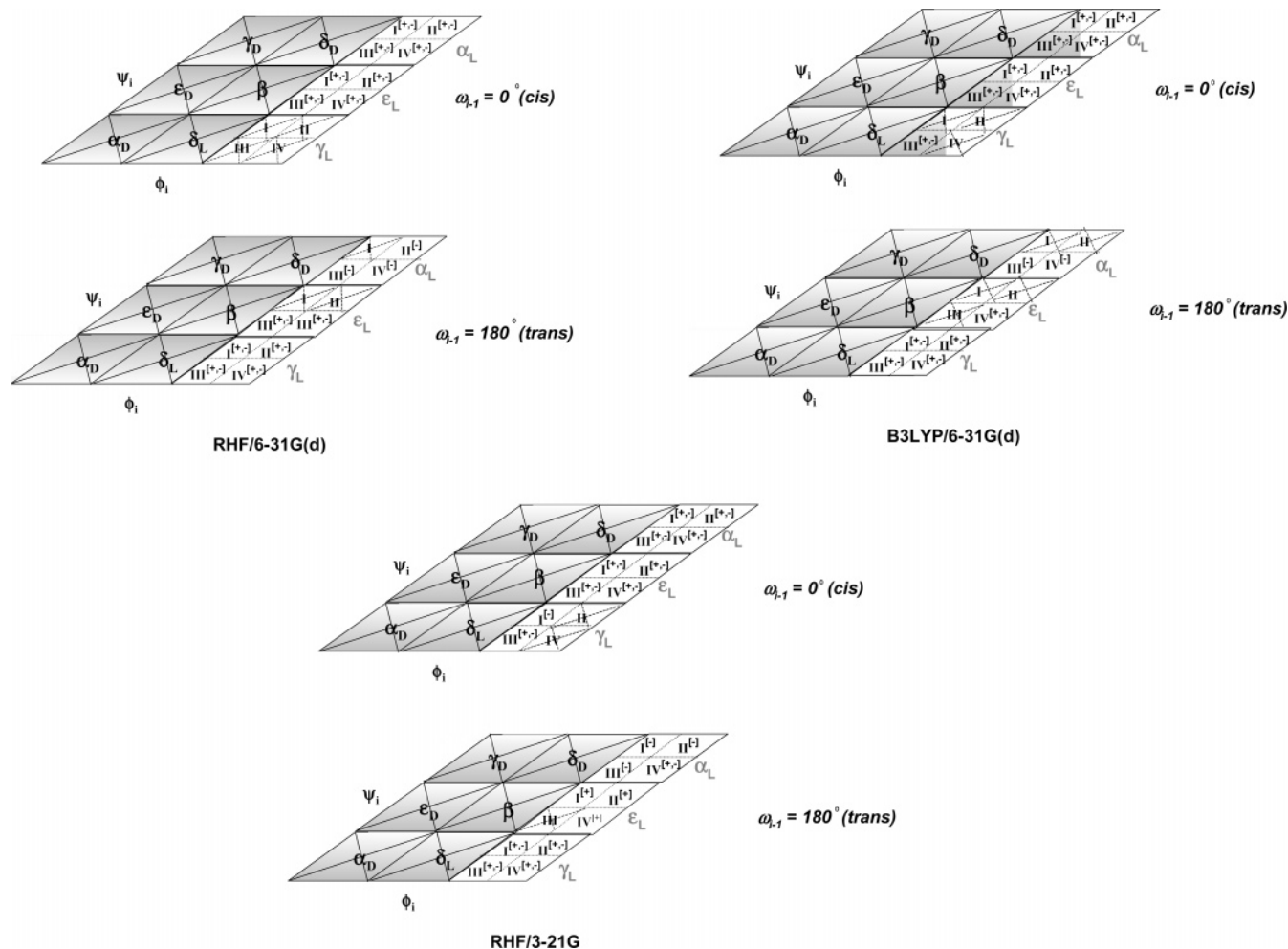


**Figure 8.** Topological representation of minima found in the  $P_N$ -CO-Pro-NH- $P_C$  family at the RHF/3-21G, RHF/6-31G(d), and B3LYP/6-31G(d) levels of theory. The ring puckerings corresponding to the  $\chi_i^1$  values are depicted within the square brackets by either + for  $\chi_i^1 = g^+$  and - for  $\chi_i^1 = g^-$ .

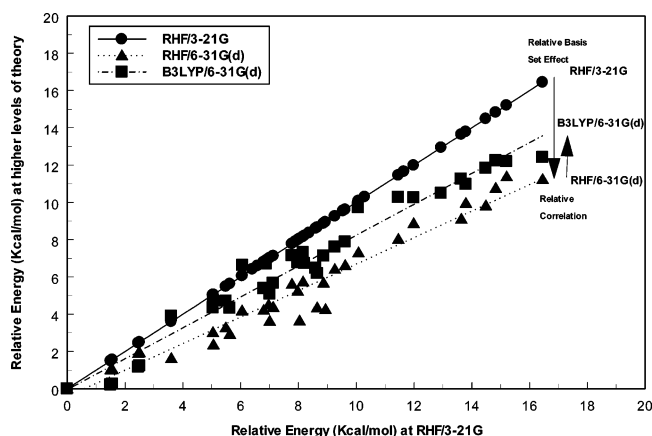


**Figure 9.** Schematic illustration of the basis set effect and electron correlation on the relative energies of existing minima computed at RHF/3-21G, RHF/6-31G(d) and B3LYP/6-31G(d) levels of theory for all  $P_N$ -CO-Pro-NH- $P_C$  compounds.

The functional variation of  $\chi_i^0$  with  $P$  at the RHF/6-31G(d) and B3LYP/6-31G(d) levels of theory is illustrated in Figure 12a and 12b, respectively. The average  $\bar{A}$  values were 37.46° and 37.56°, which are listed in the footnotes of Tables 4 and 5.

As a general observation, a cis peptide bond decreases  $\phi_i$ , increases  $A$  and the absolute value of  $P$ , and also increases  $\psi_i$  torsional angles. Ring puckerings do not considerably change trans

$\omega_i$  values but positive ring puckerings increase cis  $\omega_i$  values, decrease  $\phi_i$ , and increase both  $A$  and  $\psi_i$ .<sup>39</sup> The present results reconfirm these observations.

In Tables 3–5, the puckering amplitude  $A$  exists in a well-defined range. Hence, the maximum deviation of ring atoms from the mean plane is approximately the same for all conformers of compounds [I]–[IV]. Consequently, the phase angle,  $P$ , which ideally has a periodicity of 36°, is sufficient to describe the different ring structures of the four compounds, similar to established results.<sup>33,39,42,78</sup>

**3.3. Advanced Computations.** For the  $P_N$ -CO-Pro-NH- $P_C$  family, use of the simplest model  $P_N = P_C = H$  (compound [I]) is quite acceptable. Consequently, advanced computations were carried out only for compound [I]. Table 7 lists the energy values and Figure 13 represents a correlation of all values obtained at RHF/3-21G, RHF/6-31G(d), B3LYP/6-31G(d), CBS-4M, and G3MP2. Clearly, CBS-4M, G3MP2, and RHF/6-31G(d) show nearly identical trends, whereas the values computed at the RHF/3-21G and B3LYP/6-31G(d) levels of theory deviate substantially. The  $\Delta E$  values obtained at the RHF/3-21G, RHF/6-31G(d) and B3LYP/6-31G(d) levels of theory are ordered in Figure 13 in the same fashion as was seen in Figure 9, suggesting that the B3LYP/6-31G(d) level results are not as reliable in accounting for correlation effect like those obtained at the more advanced level of computations (CBS-4M and G3MP2).

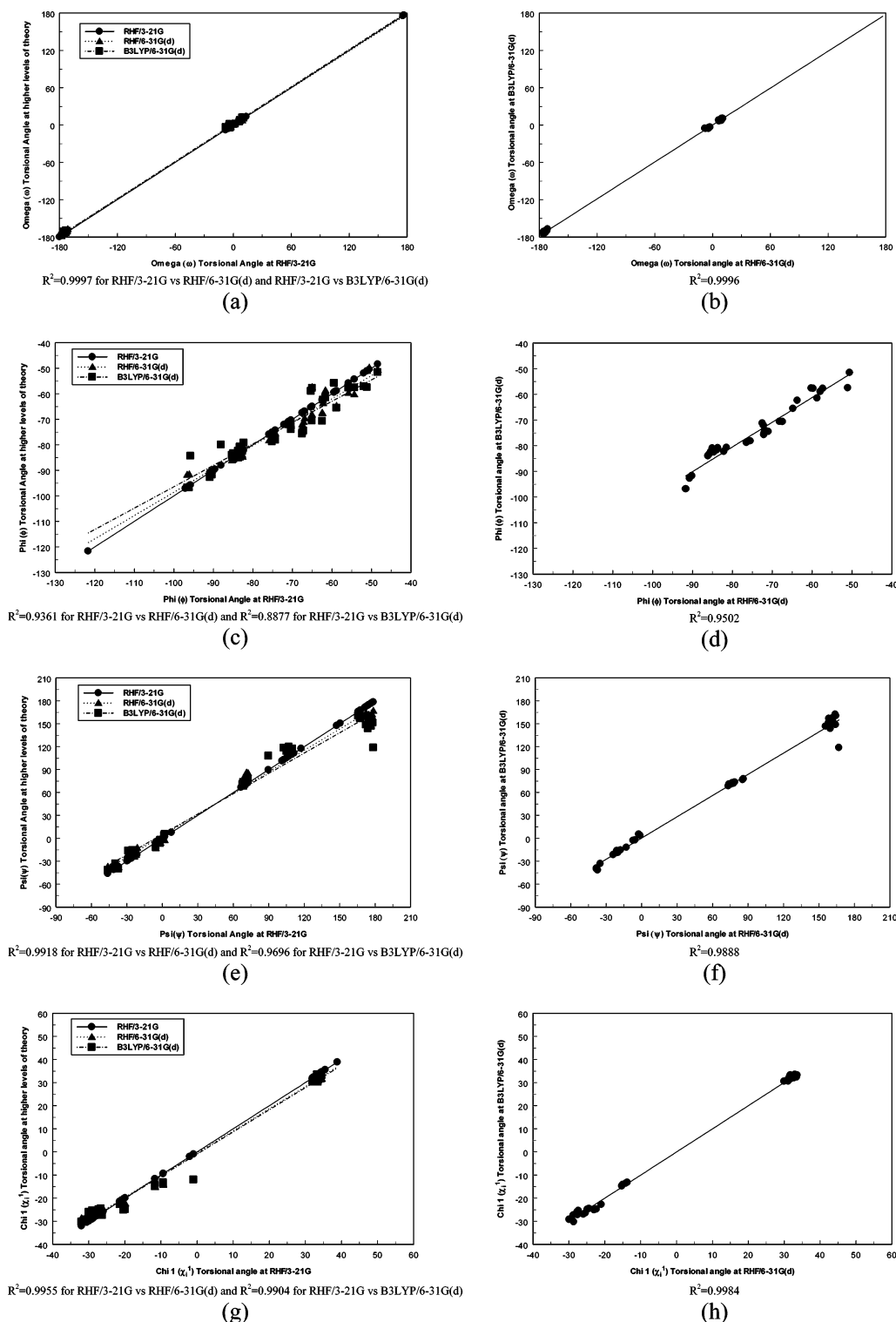


**Figure 10.** Correlation of torsional angles:  $\omega_{i-1}$  (a) and (b);  $\phi_i$  (c) and (d);  $\psi_i$  (e) and (f);  $\chi_i^1$  (g) and (h) for the  $P_N\text{--CO--Pro--NH--P}_C$  compounds obtained from geometry optimizations at three levels of theory.  $R^2$  values are also indicated.

The trends computed for the thermodynamic functions are shown in Figure 14. Both CBS-4M and the G3MP2 results produced the same trend.

#### 4. Conclusions

With the aid of a standardized numbering system, this paper has detailed a first principle computational study on the full conformational space of L-proline diamides. The study aimed to explore, characterize, and present the geometric preferences

of the  $P_N\text{--CO--Pro--NH--P}_C$  family, developed for both cis and trans isomers, at the RHF/3-21G, RHF/6-31G(d) and B3LYP/6-31G(d) levels of theory.

It was found that although the relative stabilities of minima for the four compounds ( $\text{HCO--Pro--NH}_2$ ,  $\text{MeCO--Pro--NH}_2$ ,  $\text{HCO--Pro--NH--Me}$ , and  $\text{MeCO--Pro--NH--Me}$ ), differ from each other, there are no significant differences in the overall PESs. This was seen at the RHF/3-21G level of theory from PESs and PEC.



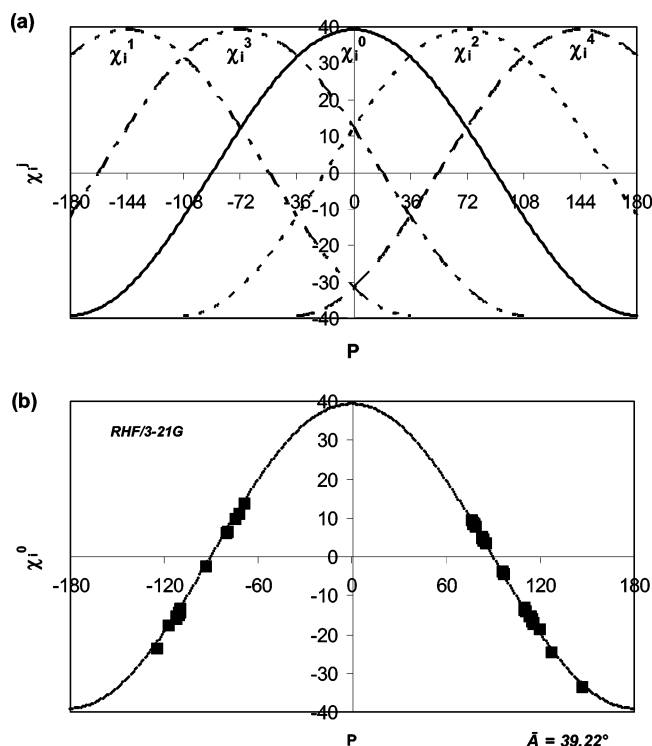


**Figure 11.** (a) Reduction of the five pseudorotational parameters  $\chi_i^0$ ,  $\chi_i^1$ ,  $\chi_i^2$ ,  $\chi_i^3$ , and  $\chi_i^4$  to  $A$  and  $P$ . (b). The functional variation of  $\chi_i^0$  with  $P$ , with computed  $\chi_i^0$  of existing minima using an  $\bar{A}$  average value as listed in the footnotes of Table 3 for the RHF/3-21G level of theory.

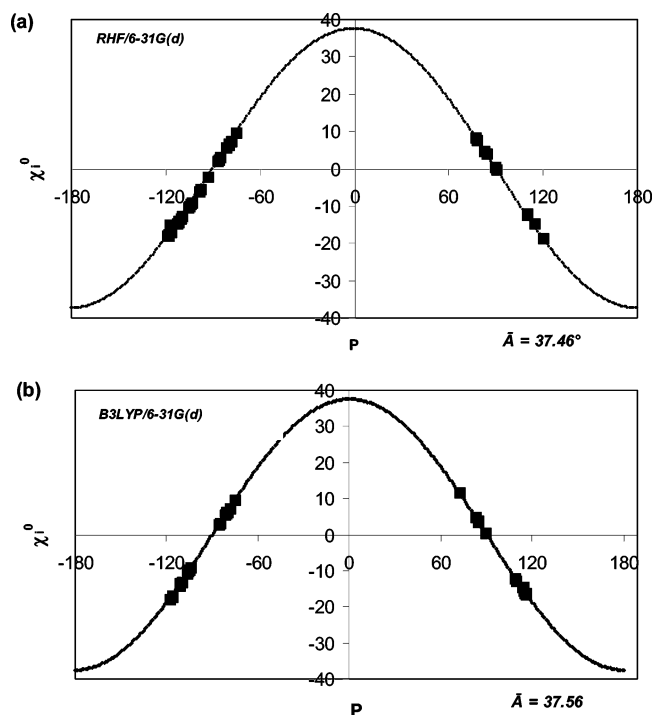


**Figure 12.** Functional variation of  $\chi_i^0$  as represented in (13);  $\chi_i^0 = \bar{A} \cos P$ . (a) and (b) show computed  $\chi_i^0$  of existing minima using an average  $\bar{A}$  value as listed in the footnotes of Tables 4 and 5 at the RHF/6-31G(d) and B3LYP/6-31G(d) level of theory, respectively.

At the RHF/6-31G(d) and B3LYP/6-31G(d) levels of theory, 41 minima were found as compared to the 50 found minima at the RHF/3-21G level of theory.

The global minimum for compounds [I] and [II] was found to be trans- $\gamma_L[+]$ ; for compounds [III] and [IV] it was also  $\gamma_L[+]$ , but in the trans-trans isomer. However, differing local

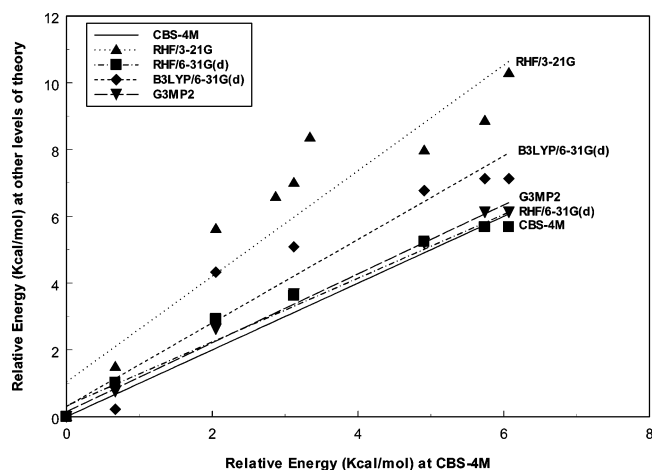


**Figure 13.** Schematic illustration of the basis set effect and electron correlation of the relative energies of existing minima at RHF/3-21G, RHF/6-31G(d), B3LYP/6-31G(d), CBS-4M, and G3MP2 levels of theory for HCO-Pro-NH<sub>2</sub>.

minima (cis  $\gamma_L[+]$ , cis-cis  $\epsilon_L[+]$ , trans-cis and trans-trans  $\gamma_L[+]$ ) were found depending on the orientation of both peptide bonds, indicating a strong relationship between peptide bond orientation and structure stability.

It should be noted that one minima stood out from the rest in the case of the cis-cis isomer of compound [III] at the RHF/3-21G level of theory, where the  $\alpha_L[+]$  conformer migrated to  $\gamma_L[+]$ , which was distorted toward a  $\delta_L[+]$  conformation.

Very good correlations of relative energies and torsional angles ( $\omega_{i-1}$ ,  $\phi_i$ ,  $\psi_i$ , and  $\chi_i^1$ ) across the three levels of theory indicate the reliability of a small basis set (i.e., RHF/3-21G) in giving a faithful representation of electron distribution that would be similarly found with a higher basis set (i.e., RHF/6-31G(d) or B3LYP/6-31G(d)). The role of correlation energy is better represented at the CBS-4M and G3MP2 levels of theory than at the B3LYP/6-31G(d) level of theory because the latter provided an overestimation of electron correlation. Also, the thermodynamic functions computed at the CBS-4M and G3MP2 levels of theory were quite comparable. Finally, the use of the simplest model, compound [I] with  $P_N = P_C = H$ , is not a misleading practice in analyzing peptide models as minor differences in geometry and stability are observed without cost of time and additional computational power.

As reported earlier, cis conformers are found in unexpectedly high proportion in folded proteins.<sup>39</sup> All ideal  $\epsilon_L$  and  $\alpha_L$  type conformers are present in both sets but negative ring puckers following cis peptide bonds are rare. The puckering amplitude,  $A$ , was found to exist in a well-defined range, whereas the phase angle,  $P$ , with an ideal periodicity of  $36^\circ$ , was sufficient enough to describe the different ring structures of the four compounds. As a general observation, a cis peptide bond decreases  $\phi_i$  while it increases  $A$ , the absolute value of  $P$ , and  $\psi_i$ . Ring puckers do not considerably change trans  $\omega_i$  values but positive ring puckers increase cis  $\omega_i$  values, decrease  $\phi_i$ , and increase<sup>39</sup> both  $A$  and  $\psi_i$ .

The results found herein for the precomputed amino acid structure of the  $P_N$ -CO-Pro-NH- $P_C$  family would be important for future investigations of larger oligopeptides. By understanding the similarities and differences of the amino acid modules, one may see how a standardized definition may be used to study larger peptides, such as Pro-Pro-Thr-Pro and Pro-Pro-Gly-Phe occurring as significant tetrapeptide segments in the antibody Immunoglobulin A1 (IgA1)<sup>60,61</sup> and Bradykinin,<sup>62,63</sup> respectively.

TABLE 7: Selected Parameters of HCO-Pro-NH<sub>2</sub> Conformers Obtained at the CBS-4M

isomer	conformer BB [SC]	energy			enthalpy			entropy	Gibbs free energy			
		total (Hartrees)	relative (kcal·mol <sup>-1</sup> )		total (Hartrees)	relative (kcal·mol <sup>-1</sup> )		total [cal/(mol K)]	total (Hartrees)	relative (kcal·mol <sup>-1</sup> )		
			$\Delta E_{\text{GL}}$	$\Delta E_{\text{LO}}$		$\Delta E_{\text{GL}}$	$\Delta E_{\text{LO}}$			$\Delta E_{\text{GL}}$	$\Delta E_{\text{LO}}$	
CBS-4M												
c	$\alpha_{\text{L}}[+]$	-494.102406	2.05	0.00	-493.926132	2.31	0.00	94.23	-493.972059	1.26	0.00	
	$\alpha_{\text{L}}[-]$	-494.100692	3.12	1.08	-493.924343	3.43	1.12	94.30	-493.970308	2.36	1.10	
	$\epsilon_{\text{L}}[-]$	-494.097846	4.91	2.86	-493.921483	5.23	2.92	94.80	-493.967688	4.00	2.74	
	$\epsilon_{\text{L}}[+]$	-494.096522	5.74	3.69	-493.920129	6.08	3.77	94.60	-493.966242	4.91	3.65	
	$\gamma_{\text{L}}[-]$	-494.096003	6.07	4.02	-493.919572	6.43	4.12	95.72	-493.966215	4.93	3.67	
t	$\alpha_{\text{L}}[-]$	-494.100347	3.34	3.34	-493.923965	3.67	3.67	94.66	-493.970106	2.48	2.48	
	$\epsilon_{\text{L}}[+]$	-494.101092	2.87	2.87	-493.924704	3.21	3.21	95.67	-493.971318	1.72	1.72	
	$\gamma_{\text{L}}[+]$	-494.105669	0.00	0.00	-493.929816	0.00	0.00	90.76	-493.974065	0.00	0.00	
	$\gamma_{\text{L}}[-]$	-494.104598	0.67	0.67	-493.928680	0.71	0.71	91.60	-493.973329	0.46	0.46	
G3MP2B3												
c	$\alpha_{\text{L}}[+]$	-494.086347	2.62	0.00	-493.913853	3.00	0.00	98.70	-493.961341	1.63	0.00	
	$\alpha_{\text{L}}[-]$	-494.084669	3.68	1.05	-493.912168	4.05	1.06	98.34	-493.959484	2.79	1.17	
	$\epsilon_{\text{L}}[+]$	-494.082260	5.19	2.56	-493.909614	5.66	2.66	100.06	-493.957747	3.88	2.26	
	$\epsilon_{\text{L}}[-]$	-494.080772	6.12	3.50	-493.908065	6.63	3.63	100.97	-493.956632	4.58	2.95	
t	$\gamma_{\text{L}}[+]$	-494.090529	0.00	0.00	-493.918627	0.00	0.00	94.16	-493.963938	0.00	0.00	
	$\gamma_{\text{L}}[-]$	-494.089341	0.75	0.75	-493.917464	0.73	0.73	94.37	-493.962870	0.67	0.67	

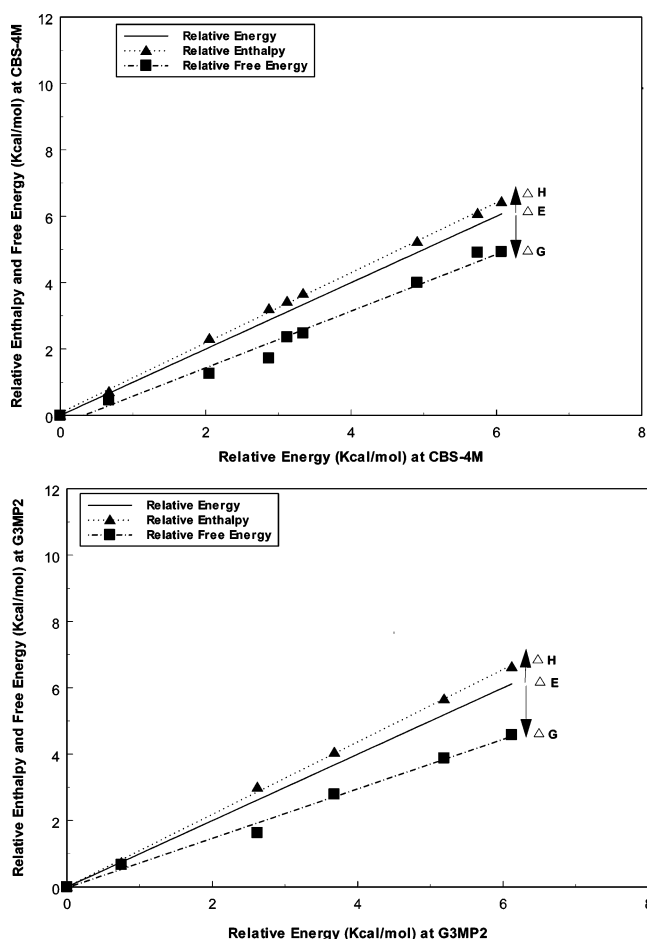


**Figure 14.** Schematic illustration of the dependence of the relative thermodynamic functions on for the existing minima computed at the CBS-4M and G3MP2 levels of theory for HCO-Pro-NH<sub>2</sub> [I].

**Acknowledgment.** We thank the Center for Molecular Design and Information Technology (MDIT), Leslie Dan Faculty of Pharmacy, University of Toronto, as well as the Interuniversity Consortium (CINECA) in Bologna, Italy, for providing computation time. M.A.S. especially thanks Professor Andrea Bottoni for his scientific inspiration during her time at the University of Bologna. I.G.C. thanks the Ministry of Education for a Szent-Györgyi Visiting Professorship. We

gratefully thank Suzanne K. Lau, Jacqueline M. S. Law, Michael R. Sahai, Tamás Beke, András Lang, and Shekeb Kahn for their kind help while preparing this manuscript. The research described was supported partially by grants from the Hungarian Scientific Research Fund (F037648 and T046861) and the Global Institute of Computational Molecular and Materials Science (GIOCOMMS), Toronto, Ontario, Canada, allowing travel and exchange.

## References and Notes

- (1) Vitagliano, L.; Berisio, R.; Mastrangelo, A.; Mazzarella, L.; Zagari, A. *Protein Sci.* **2001**, *10*, 2627.
- (2) Richardson, J. S.; Richardson, D. C. *Science* **1988**, *240*, 1648.
- (3) MacArthur, M.; Thornton, J. M. *J. Mol. Biol.* **1991**, *218*, 397.
- (4) Martin, R.; Waldmann, L.; Kaplan, D. L. *Biopolymers* **2003**, *70*, 435.
- (5) McDonald, Q. D.; Still, W. C. *J. Org. Chem.* **1996**, *61*, 1385.
- (6) Richardson; Richardson. In *Prediction of Protein Structure and the Principles of Protein Conformation*; Fasman, G. D., Ed.; Plenum: New York, 1989; pp 1–98.
- (7) Kim, M. K.; Kang, Y. K. *Protein Sci.* **1999**, *8*, 1492.
- (8) Barlow, D. J.; Thornton, J. M. *J. Mol. Biol.* **1988**, *201*, 601.
- (9) Gibbs, A. C.; Bjorndahl, T. C.; Hodges, R. S.; Wishart, D. S. *J. Am. Chem. Soc.* **2002**, *124*, 1203.
- (10) Quancard, J.; Karoyan, P.; Lequin, O.; Wenger, E.; Aubry, A.; Lavielle, S.; Chassaing, G. *Tetrahedron Lett.* **2004**, *45*, 623.
- (11) Némethy, G.; Printz, M. P. *Macromolecules* **1972**, *6*, 755.
- (12) Guruprasad, K.; Rajkumar, S. *J. Biosci.* **2000**, *25*, 143.
- (13) Chang, D. K.; Cheung, S. F.; Trivedi, V. D.; Lin, K. L. *J. Struct. Biol.* **1999**, *128*, 270.
- (14) Wess, J.; Nanavati, S.; Vogel, Z.; Maggio, R. *EMBO J.* **1993**, *12*, 331.
- (15) Vanhoof, G.; Goossens, F.; De Meester, I.; Hendriks, D.; Scharpé, S. *FASEB J.* **1995**, *9*, 736.
- (16) Kayushina, R. L.; Vainstein, B. K. *Sov. Phys. Crystallogr.* **1966**, *10*, 698.
- (17) Balasubramanian, R.; Lakshminarayanan, A. V.; Sabesan, M. N.; Tegoni, G.; Venkatesan, K. Ramachandran, G. N. *Int. J. Pept. Protein Res.* **1971**, *3*, 25.
- (18) DeTar, D. F.; Luthra, N. P. *J. Am. Chem. Soc.* **1977**, *99*, 1232.
- (19) Westhof, E.; Sundaralingam, M. *J. Am. Chem. Soc.* **1983**, *105*, 970.
- (20) Balaji, V. N.; Rao, M. J.; Rao, S. N.; Dietrich, S. W.; Sasisekharan, V. *Biochem. Biophys. Res. Commun.* **1986**, *140*, 895.
- (21) Milner-White, E. J.; Bell, L. H.; MacCallum, P. H. *J. Mol. Biol.* **1992**, *228*, 725.
- (22) Madison, V.; Kopple, K. D. *J. Am. Chem. Soc.* **1980**, *102*, 4855.
- (23) Haasnoot, C. A. G.; De Leeuw, F. A. A. M.; De Leeuw, H. P. M.; Altona, C. *Biopolymers* **1981**, *20*, 1211.
- (24) Beausoleil, E.; Lubell, W. D. *J. Am. Chem. Soc.* **1996**, *118*, 12902.
- (25) Falk, M.; Sidhu, P.; Walter, J. A. *Nat. Toxins* **1998**, *6*, 159.
- (26) Herlinger, A. W.; Long II, T. V. *J. Am. Chem. Soc.* **1970**, *92*, 6481.

- (27) Reva, I. D.; Stepanian, S. G.; Plokhhotnichenko, A. M.; Radchenko, E. D.; Sheina, G. G.; Blagoi, Yu. P. *J. Mol. Struct.* **1994**, *318*, 1.
- (28) Zimmerman, S. S.; Pottle, M. S.; Némethy, G.; Scheraga, H. A. *Macromolecules* **1977**, *10*, 1.
- (29) Vásquez, M.; Némethy, G.; Scheraga, H. A. *Macromolecules* **1983**, *16*, 1043.
- (30) Rosas, R. L.; Cooper, C.; Laane, J. *J. Phys. Chem.* **1990**, *94*, 1830.
- (31) Némethy, G.; Gibson, K. D.; Palmer, K. A.; Yoon, C. N.; Paterlini, G.; Zagari, A.; Rumsey, S.; Scheraga, H. A. *J. Phys. Chem.* **1992**, *96*, 6472.
- (32) Fischer, S.; Dunbrack Jr., R. L.; Karplus, M. *J. Am. Chem. Soc.* **1994**, *116*, 11931.
- (33) Ramek, M.; Kelterer, A. M.; Teppen, B. J.; Schafer, L. *J. Mol. Struct. (THEOCHEM)* **1995**, *352*, 59.
- (34) Kang, Y. K. *J. Phys. Chem.* **1996**, *100*, 11589.
- (35) Baldoni, H. A.; Rodriguez, A. M.; Zamarbide, G.; Enriz, R. D.; Farkas, Ö.; Csaszar, P.; Torday, L. L.; Sosa, C. P.; Jakli, I.; Perczel, A.; Hollosi, M.; Csizmadia, I. G. *J. Mol. Struct. (THEOCHEM)* **1999**, *465*, 79.
- (36) Jhon, J. S.; Kang, Y. K. *J. Phys. Chem. A* **1999**, *103*, 5436.
- (37) Marino, T.; Russo, N.; Tocci, E.; Toscano, M. *J. Mass Spectrom.* **2001**, *36*, 301.
- (38) Benzi, C.; Improta, R.; Scalmani, G.; Barone, V. *J. Comput. Chem.* **2002**, *23*, 341.
- (39) Hudaky, I.; Baldoni, H. A.; Perczel, A. *J. Mol. Struct. (THEOCHEM)* **2002**, *582*, 233.
- (40) Improta, R.; Mele, F.; Crescenzi, O.; Benzi, C.; Barone, V. *J. Am. Chem. Soc.* **2002**, *124*, 7857.
- (41) Kang, Y. K.; Park, H. S. *J. Mol. Struct. (THEOCHEM)* **2002**, *593*, 55.
- (42) Czinki, E.; Császár, A. G. *Chem. Eur. J.* **2003**, *9*, 1008.
- (43) Hudaky, I.; Perczel, A. *J. Mol. Struct. (THEOCHEM)* **2003**, *630*, 135.
- (44) Lam, J. S. W.; Koo, J. C. P.; Hudáky, I.; Varro, A.; Papp, J. Gy.; Penke, B.; Csizmadia, I. G. *J. Mol. Struct. (THEOCHEM)* **2003**, *666–667*, 285.
- (45) Zamarbide, G. N.; Estrada, M. R.; Zamora, M. A.; Torday, L. L.; Enriz, R. D.; Vert, F. T.; Csizmadia, I. G. *J. Mol. Struct. (THEOCHEM)* **2003**, *666–667*, 599.
- (46) Allen, W. D.; Czinki, E.; Császár, A. G. *Chem. Eur. J.* **2004**, *10*, 4512.
- (47) Kang, Y. K. *J. Phys. Chem. B* **2004**, *108*, 5463.
- (48) Kang, Y. K. *J. Mol. Struct. (THEOCHEM)* **2004**, *675*, 37.
- (49) Kang, Y. K.; Choi, H. Y. *Biophys. Chem.* **2004**, *111*, 135.
- (50) Peterson, M. R.; Csizmadia, I. G. *Prog. Theor. Org. Chem.* **1982**, *3*, 10.
- (51) Mezey, P. G. *Potential Energy Hypersurfaces*; Elsevier: Amsterdam, 1987.
- (52) Perczel, A.; Ángyán, J. G.; Kajtár, M.; Viviani, W.; Rivail, J. L.; Marcoccia, J. F.; Csizmadia, I. G. *J. Am. Chem. Soc.* **1991**, *113*, 6256.
- (53) Chass, G. A.; Sahai, M. A.; Law, J. M. S.; Lovas, S.; Farkas, Ö.; Perczel, A.; Csizmadia, I. G. *Int. J. Quantum Chem.* **2002**, *90*, 933.
- (54) Sahai, M. A.; Lovas, S.; Chass, G. A.; Penke, B.; Csizmadia, I. G. *J. Mol. Struct. (THEOCHEM)* **2003**, *666–667*, 169.
- (55) Borics, A.; Chass, G. A.; Csizmadia, I. G.; Murphy, R. F.; Lovas, S. *J. Mol. Struct. (THEOCHEM)* **2003**, *666–667*, 355.
- (56) Topol, I. A.; Burt, S. K.; Deretey, E.; Tang, T.; Perczel, A.; Rashin, A.; Csizmadia, I. G. *J. Am. Chem. Soc.* **2001**, *123*, 6054.
- (57) Levitt, M. *Biochemistry* **1978**, *17*, 4277.
- (58) Lifson, S.; Sander, C. *Nature* **1979**, *282*, 109.
- (59) O' Neill, K. T.; DeGrado, W. F. *Science* **1990**, *250*, 646.
- (60) Siemion, I. Z.; Pedyczak, A.; Burton, J. *Biophys. Chem.* **1988**, *31*, 35.
- (61) Burton, J.; Wood, S. G.; Pedyczak, A.; Siemion, I. Z. *Biophys. Chem.* **1989**, *33*, 39.
- (62) Hasan, A. A.; Amenta, S.; Schmaier, A. H. *Circulation* **1996**, *94*, 517.
- (63) Stewart, J. M.; Gera, L.; Chan, D. C.; Bunn, P. A.; York, E. J.; Simkeviciene, V.; Helfrich, B. *Can. J. Phys. Pharm.* **2002**, *80*, 275.
- (64) Fejer, S. N.; Jenei, Z. A.; Paragi, G. *J. Mol. Struct. (THEOCHEM)* **2003**, *666–667*, 303.
- (65) Pal, D.; Chakrabarti, P. *J. Mol. Biol.* **1999**, *294*, 271.
- (66) Madison, V.; Schellman, J. *Biopolymers* **1970**, *9*, 65.
- (67) Frisch, M. J.; Trucks, G. W.; Schlegel, H. B.; Scuseria, G. E.; Robb, M. A.; Cheeseman, J. R.; Montgomery, J. A., Jr.; Vreven, T.; Kudin, K. N.; Burant, J. C.; Millam, J. M.; Iyengar, S. S.; Tomasi, J.; Barone, V.; Mennucci, B.; Cossi, M.; Scalmani, G.; Rega, N.; Petersson, G. A.; Nakatsuji, H.; Hada, M.; Ehara, M.; Toyota, K.; Fukuda, R.; Hasegawa, J.; Ishida, M.; Nakajima, T.; Honda, Y.; Kitao, O.; Nakai, H.; Klene, M.; Li, X.; Knox, J. E.; Hratchian, H. P.; Cross, J. B.; Adamo, C.; Jaramillo, J.; Gomperts, R.; Stratmann, R. E.; Yazyev, O.; Austin, A. J.; Cammi, R.; Pomelli, C.; Ochterski, J. W.; Ayala, P. Y.; Morokuma, K.; Voth, G. A.; Salvador, P.; Dannenberg, J. J.; Zakrzewski, V. G.; Dapprich, S.; Daniels, A. D.; Strain, M. C.; Farkas, O.; Malick, D. K.; Rabuck, A. D.; Raghavachari, K.; Foresman, J. B.; Ortiz, J. V.; Cui, Q.; Baboul, A. G.; Clifford, S.; Cioslowski, J.; Stefanov, B. B.; Liu, G.; Liashenko, A.; Piskorz, P.; Komaromi, I.; Martin, R. L.; Fox, D. J.; Keith, T.; Al-Laham, M. A.; Peng, C. Y.; Nanayakkara, A.; Challacombe, M.; Gill, P. M. W.; Johnson, B.; Chen, W.; Wong, M. W.; Gonzalez, C.; Pople, J. A. *Gaussian 03*, revision B.01; Gaussian, Inc.: Pittsburgh, PA, 2003.
- (68) Kilpatrick, J. E.; Pitzer, K. S.; Spitzer, R. *J. Am. Chem. Soc.* **1947**, *69*, 2483.
- (69) Geise, H. J.; Altona, C.; Romers, C. *Tetrahedron Lett.* **1967**, *15*, 1383.
- (70) Altona, C.; Sundaralingam, M. *J. Am. Chem. Soc.* **1972**, *94*, 8205.
- (71) Dunitz, J. D. *Tetrahedron* **1972**, *28*, 5459.
- (72) Cremer, D.; Pople, J. A. *J. Am. Chem. Soc.* **1975**, *97*, 1354.
- (73) Chacko, K. K.; Swaminathan, S.; Veena, K. R. *Curr. Science* **1983**, *52*, 660.
- (74) Pfafferoth, G.; Oberhammer, H.; Boggs, J. E.; Caminati, W. *J. Am. Chem. Soc.* **1985**, *107*, 2305.
- (75) Tomimoto, M.; Go, N. *J. Phys. Chem.* **1995**, *99*, 563.
- (76) Han, S. J.; Kang, Y. K. *J. Mol. Struct. (THEOCHEM)* **1996**, *362*, 243.
- (77) Han, S. J.; Kang, Y. K. *J. Mol. Struct. (THEOCHEM)* **1996**, *369*, 157.
- (78) Carballeira, L.; Pérez-Juste, I. *J. Chem. Soc., Perkin Trans.* **1998**, *2*, 1339.
- (79) Kang, Y. K.; Jhon, J. S.; Han, S. J. *J. Pep. Res.* **1999**, *53*, 30.
- (80) Petersson, G. A.; Al-Laham, M. A. *J. Chem. Phys.* **1991**, *94*, 6081.
- (81) Petersson, G. A.; Tensfeldt, T.; Montgomery, J. A. *J. Chem. Phys.* **1991**, *94*, 6091.
- (82) Montgomery, J. A.; Frisch, M. J.; Ochterski, J. W.; Petersson, G. A. *J. Chem. Phys.* **2000**, *112*, 6532.
- (83) Curtiss, L. A.; Raghavachari, K.; Redfern, P. C.; Rassolov, V.; Pople, J. A. *J. Chem. Phys.* **1998**, *109*, 7764.
- (84) Baboul, A. G.; Curtiss, L. A.; Redfern, P. C.; Raghavachari, K. *J. Chem. Phys.* **1999**, *110*, 7650.
- (85) Curtiss, L. A.; Redfern, P. C.; Raghavachari, K.; Rassolov, V.; Pople, J. A. *J. Chem. Phys.* **1999**, *110*, 4703.